# Structure and Dynamics of a Tropical Squall-Line System<sup>1</sup>

ROBERT A. HOUZE, JR.

Department of Atmospheric Sciences, University of Washington, Seattle 98195 (Manuscript received 13 June 1977, in final form 1 September 1977)

#### ABSTRACT

A tropical squall-line system which moved over the observational network of the Global Atmospheric Research Programme's Atlantic Tropical Experiment (GATE) was investigated using rawinsonde, weather radar, satellite, surface meteorological, acoustic sounder and cloud photographic data. Combining these data led to a detailed synthesis of the three-dimensional structure, dynamics and life cycle of the disturbance.

The squall-line system consisted of a squall line forming the leading edge of the system and a trailing anvil cloud region. The squall line was made up of discrete active centers of cumulonimbus convection, referred to as line elements (LE's). New LE's formed ahead of the squall line. Old LE's weekened toward the rear of the line and blended into the trailing anvil region as they dissipated. Each LE progressed through a period of rapid growth, with echo tops penetrating the tropopause to maximum heights of 16-17 km, then decreasing to heights of 13-14 km, which corresponds to the height of the anvil cloud with which the LE's merged at the end of their lifetimes.

The squall line was located along the leading edge of a mesoscale downdraft forming and spreading out in the middle and lower troposphere below the anvil cloud. Within the squall line, individual LE's contained smaller, convective-scale downdrafts which penetrated down to the sea surface. This cold, convective-scale downdraft air spread out at low levels providing lift for the updraft on the leading side of the LE. The convective-scale downdraft air also spread out in a layer 200-400 m deep toward the rear of the system. The top of this layer of cold air was bounded by a stable layer below which enhanced turbulent mixing occurred.

Precipitation falling from the trailing anvil cloud was stratiform and accounted for 40% of the total rain from the squall-line system. Thus, much of the anvil cloud is accounted for by the successive incorporation of weakened, but precipitation-laden old LE's from the back edge of the squall line and possibly by widespread upward air motion within the upper level anvil cloud.

### 1. Introduction

Tropical squall lines (or disturbance lines, as they are sometimes called) were first brought to the attention of the scientific community in vivid descriptions by meteorologists concerned with weather forecasting in West Africa (Hamilton and Archbold, 1945; Eldridge, 1957; Tschirhart, 1958). Working with conventional synoptic data, pilot reports and careful observations of the state of the sky, Hamilton and Archbold (1945) deduced that a typical tropical squall line consists of a row of cumulonimbus clouds forming at the edge of a broad downdraft region. They noted that the downdraft region is located under a precipitating trailing anvil cloud which emanates from the cumulonimbus towers and that "a sudden squall from between southeast and northeast" accompanied by a frontal-like temperature drop typically precedes the downpour of rain from the row of cumulonimbus clouds by just 2 or 3 min. This squall front is "the last warning to take cover" and marks the edge of cold downdraft air, which spreads under the warm air ahead of the system and generates the uplift for the line of cumulonimbus clouds.

From data obtained during the Line Islands Experiment, Zipser (1969) found that the region influenced by the trailing downdraft region of a tropical squall-line system<sup>2</sup> reached a width of 600 km. More recently, Zipser (1977) has proposed that two distinct types of downdrafts occupy the trailing region of a tropical squall-line system. Intense, convective-scale downdrafts occur in the narrow (10–20 km wide) heavy precipitation zone of the squall line itself, while a more gentle, but broader (100–500 km wide), mesoscale downdraft

<sup>&</sup>lt;sup>1</sup> Contribution No. 434, Department of Atmospheric Sciences, University of Washington.

<sup>&</sup>lt;sup>2</sup> In this paper, the term squall line refers to the line of cumulonimbus clouds and heavy precipitation forming along the downdraft squall front. The term squall-line system refers to the entire disturbance consisting of the squall line, its trailing anvil cloud, the squall front, downdrafts and all associated precipitation.

forms in the precipitation region below the trailing anvil cloud.

The convective-scale downdrafts are presumed to be negatively buoyant features composed of air initially dragged downward by the weight of precipitation particles, then cooled by evaporation. This mechanism, first suggested by Brooks (1922) and later elaborated by Byers and Braham (1949, pp. 24, 41–42), produces convective-scale downdrafts in one-, two- and three-dimensional models of cumulonimbus clouds (e.g., Ogura and Takahashi, 1971; Takeda, 1971; Wilhelmson, 1974; Miller and Pearce, 1974).

The mesoscale downdraft of a tropical squall-line system was envisaged by Zipser (1969) to be driven by widespread cooling due to the evaporation of precipitation below the base of the mesoscale trailing anvil cloud. Using a hydrostatic, unfiltered numerical model, in which both cumulus-scale convection and cloud microphysical processes are parameterized, Brown (1974) demonstrated that this mechanism is feasible. In his model, the mesoscale descent is sufficiently strong to transport midtropospheric air to lower levels and is associated with a weak, but realistic mesohigh. Observations of shallow layers of apparent warming between 700 and 800 mb below the anvils of convective storms over Venezuela, however, have recently led Miller and Betts (1977) to question whether the mesoscale downdraft is evaporatively driven or forced by some other mechanism.

Generally, the overall squall-line airflow pattern proposed and later refined by Zipser (1969, 1977) is supported by the results of Obasi (1974) and Betts et al. (1976) who, by compositing rawinsonde data, derived the mean flow in the vicinity of tropical squall lines. These mean air motions are the result of a complex interaction of convective and mesoscale components of the squall-line system, some of which have time and space scales smaller than those of the system as a whole. If the convection associated with tropical squall lines and its interaction with the large-scale environment are to be accurately modeled and parameterized, precise and detailed descriptions on all scales, extending down to the scale of individual cumulonimbus cells, are needed. Important unanswered questions include the following:

- To what extent do tropical squall lines consist of discrete active centers of convection, and to what extent do they exhibit true two-dimensionality?
- Do tropical squall lines move by translation or by preferential development on the leading side of the line?
- What is the vertical structure of the convective towers in a squall line; do they exhibit any slope in the vertical?
- Is the trailing anvil region and its associated precipitation stratiform in character, or is there some convection embedded in this region?

- Does the anvil cloud consist of cumulonimbus debris or is it dynamically active?
- How does the structure of the squall line system vary over its lifetime?

In the present study, all of these questions are addressed for the tropical squall line which passed through the data network of the Global Atmospheric Research Program's Atlantic Tropical Experiment (GATE) during the period 4–5 September 1974. This paper focuses on the cloud and precipitation fields of the squall-line system. However, since the aim is to provide insight into the dynamics of the squall-line system, the wind and thermodynamic fields are also examined and related to the observed cloud and precipitation structure.

The squall-line system examined in this paper was one of four observed by the author while serving as Radar Scientist on board the U. S. Ship Researcher during Phase III of GATE from 30 August–19 September 1974 (Houze, 1975, 1976). The importance of understanding the dynamics of these disturbances and their role in the general circulation and energetics of the tropical atmosphere is illustrated by the fact that these four squall lines accounted for 50% of the rain recorded on board the Researcher during Phase III of GATE.

### 2. Data

### a. Radar observations

The data which made it possible to examine the substructure of the 4-5 September 1974 squall-line system are the three-dimensional, digitially processed and recorded, quantitative radar data collected during GATE. The capability of the GATE radars to probe large volumes of the atmosphere with high spatial and temporal resolution made them especially effective for revealing the internal structure of large tropical cloud systems. Radar beams can penetrate throughout the region under the upper-level cirrus shield of a cloud system seen in a satellite picture and reflect a vivid picture of the inner workings of the cloud system. A long-encountered problem in radar meteorology, however, has been the absence of suitable means for rapid recording of radar echo patterns at the time that they are observed in a form practicable for extensive later analysis. In GATE, this obstacle was overcome through the use of modern radar signal processing and digital recording techniques (Hudlow, 1975a,b). The resulting digital data are readily used as input to computer programs which generate displays of the observed echo patterns in a variety of formats which facilitate the analysis of large quantities of data. For this paper, over 1000 vertical and horizontal cross sections through echocovered regions of the atmosphere were generated and used to examine the precipitation intensity, threedimensional structure, horizontal motion and life

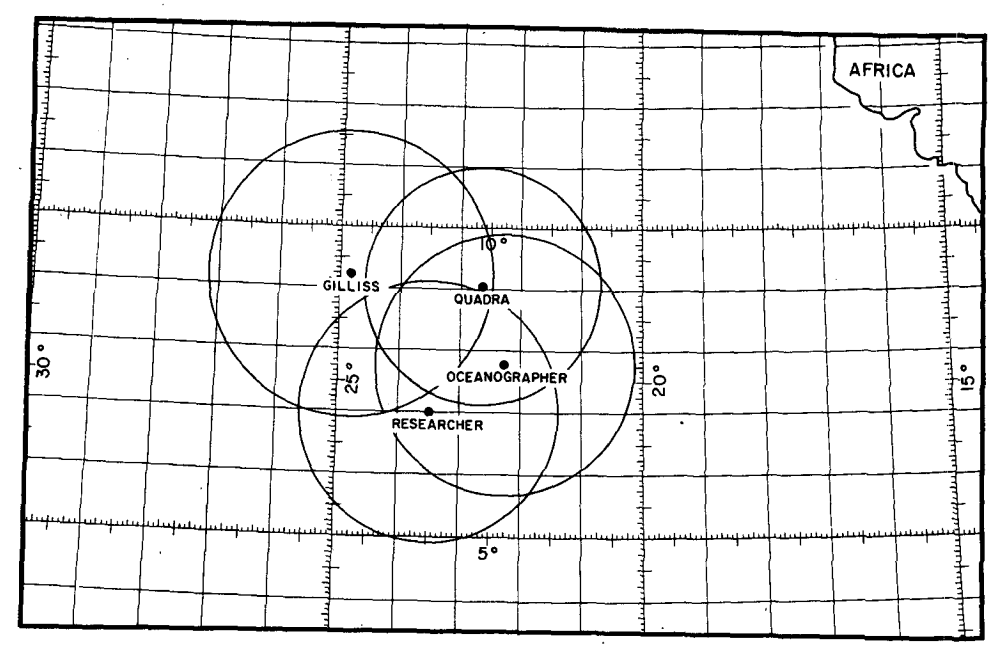


Fig. 1. Positions of ships carrying quantitative radars during Phase III of GATE (30 August-10 September 1974).

history of each important precipitation entity associated with the squall-line system.

# b. The GATE shipboard radar systems

Radar systems were deployed on board four GATE ships (Fig. 1). The characteristics of these shipboard radar systems are summarized in Table 1. The Ocean-ographer and Researcher radar systems are described in detail by Hudlow (1975a,b, 1976a,b,c). The Gilliss and Quadra radar systems are described by P. M. Austin (1976a,b,c). and G. L. Austin (1977), respectively.

At all four radars a three-dimensional scanning routine was commenced simultaneously every 15 min throughout GATE. The antenna of each radar swept through 360° in azimuth for a series of elevation angles ranging from 0° to 22°. Signals returned to the radar on each sweep were processed and recorded both digitally and photographically on board the ships. A set of three-dimensional scans took about 5 min to complete, leaving a 10 min period before the initiation of the next three-dimensional scan period. On the Oceanographer and Researcher, additional data were

TABLE 1. Characteristics of GATE shipborne weather radar systems.

Radar	Ships						
characteristics	Gilliss	Oceanographer	Researcher	Quadra			
Wavelength (cm)	5.30	5.30	5.35	5.35			
Peak power (kW)	250	215	225	1000			
Beamwidth (deg)	1.45	1.5	2.0	1.0			
Range bin size (km)	0.25-1.00	2	2.0	1.0			
Azimuth recording increment (deg)	1	2	2	1			

collected during the 10 min interim by photographing base-level (generally 0-0.6° elevation angle) PPI (Plan Position Indicator) displays at 5 min intervals. The resulting time-lapse movies aided greatly in establishing continuity between the three-dimensional scans recorded digitally once every 15 min.

In this study, data from all four GATE quantitative radars were used. Without their overlapping coverage it would not have been possible to examine the 4-5 September squall-line system in its entirety.

### c. Satellite data

During the summer of 1974, the synchronous meteorological satellite SMS-1 was positioned especially to provide detailed imagery over the GATE area. These data were obtained at 15–30 min intervals throughout the experiment, providing a detailed history of the development of the upper level (and to some extent lower level) cloud structure associated with the precipitation field seen in the radar data. Combining the satellite data with the three-dimensional radar data gives a full picture of the overall cloud and precipitation structure associated with the squall-line system.

During daylight hours both visible imagery, with a horizontal resolution of 0.92 km, and infrared imagery, with a horizontal resolution of 7.4 km, were obtained from the SMS-1 satellite. The infrared observations were continued throughout the night. For this study, gridded SMS-1 photographs and film loops were obtained through the *GATE Data Catalogue* (EDS, 1975), and special photographic data and contoured maps of the SMS-1 brightness intensity patterns for both infrared and sun-angle normalized visible images were

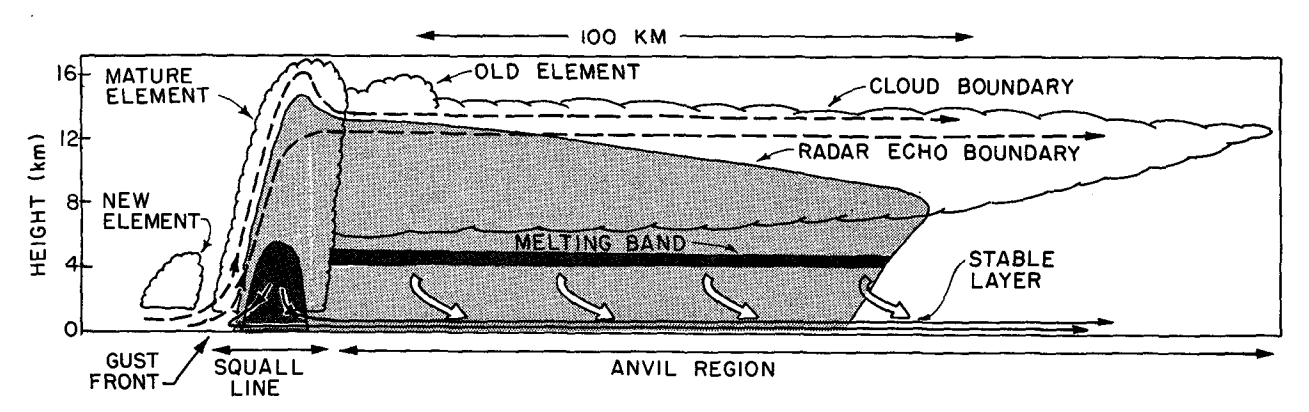


Fig. 2. Schematic cross section through squall-line system. Streamlines show flow relative to the squall line. Dashed streamlines show updraft circulation, thin solid streamlines show convective-scale downdraft circulation associated with mature squall-line element, and wide arrows show mesoscale downdraft below the base of the anvil cloud. Dark shading shows strong radar echo in the melting band and in the heavy precipitation zone of the mature squall-line element. Light shading shows weaker radar echoes. Scalloped line indicates visible cloud boundaries.

prepared by the Space Science and Engineering Center at the University of Wisconsin.

## d. Upper air data

In this study, GATE upper air observations (EDS, 1975) are referred to both in the form in which they were first transmitted [the "Quick Look" and "Quick Look (Supplementary)" Data Sets] and in their more recently prepared "Nationally Processed and Validated" form. The latter, described by Acheson (1976), includes wind, temperature and humidity measurements at 5 mb intervals, while the former included only standard and significant pressure levels.

### e. Acoustic sounder data

The structure of the atmospheric boundary layer in the vicinity of the GATE 4-5 September squall line was documented by an acoustic echo sounder system on board the *Oceanographer*. The instrumentation has been described by Mandics *et al.* (1975) and Mandics and Hall (1976). The data are available through the *GATE Data Catalogue* (EDS, 1975).

### f. Surface data

Synoptic surface observations used in this study were taken from the Quick Look and Quick Look (Supplementary) Data Sets and from microfilm records of 3 min averages of temperature, humidity, wind and radiation measured continuously on board the Oceanographer and Researcher (EDS, 1975). Records of raingage measurements made at one-half to one-hour intervals on board the Oceanographer and Researcher were supplied by the NOAA Center for Experiment Design and Data Analysis.

# g. Ship-based cloud photography

This study used all-sky camera movies taken on board U. S. ships (EDS, 1975). Panoramic photographs of cloud patterns on the horizon as viewed from the Oceanographer and Researcher were supplied by GATE scientists at the University of Virginia. Cloud photographs were taken by the author on board the Researcher.

## h. Aircraft Data

No GATE research flights were made in the 4-5 September squall-line system.

#### 3. Schematic illustration of squall-line structure

A synthesis of the conclusions of this study is shown in Fig. 2. This schematic illustration depicts the structural and dynamical features of the GATE 4–5 September squall-line system. It is presented here so that it may be used as a point of reference in visualizing the results of the following sections.

### 4. Formation of the squall-line system

The formation of the GATE 4-5 September squall line is illustrated in the sequence of infrared satellite pictures shown in Fig. 3. At 0800³ on 4 September, the dark region located between the arrows in Fig. 3a contained no evidence of cloudiness. At 1000, two small dots of upper level cloud were evident at the ends of the arrows in Fig. 3b. These small areas of high cloud, which were the tops of growing cumulonimbus towers, were the first evidence of convection associated with the squall line. By 1200, the two cloud tops had expanded and begun to merge, forming a continuous upper level cloud shield which was quite large by 1400 (Figs. 3 and 3d).

The large dissipating cloud feature immediately to the northeast of the dark region indicated by arrows at 0800 in Fig. 3a had moved from northeast to southwest over the ocean from a position over the African

<sup>&</sup>lt;sup>3</sup> All times are GMT.

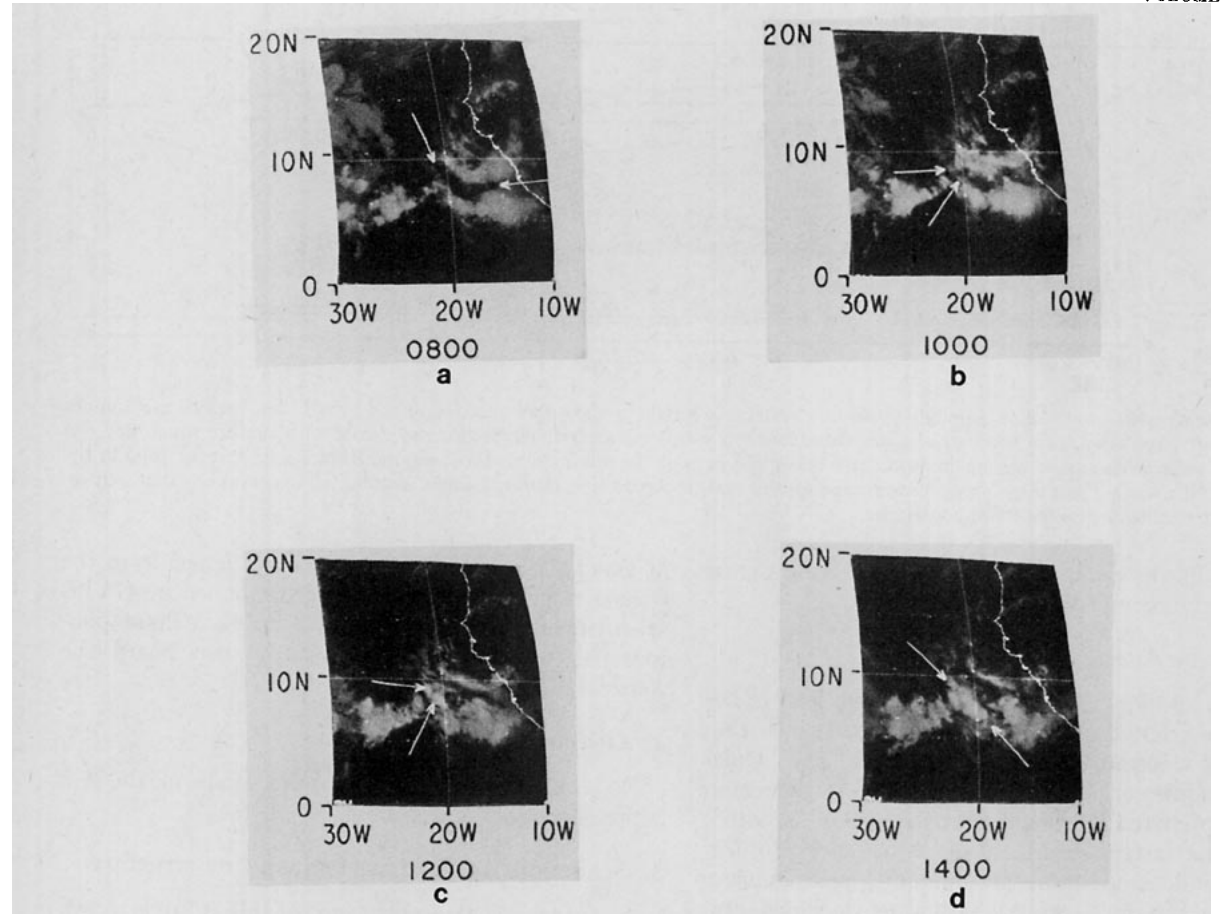


Fig. 3. Sequence of SMS-1 infrared satellite pictures showing formation of squall line on 4 September 1974. Times are GMT. Arrows indicate features referred to in text.

continent on the preceding day. The new squall line evidently formed ahead of and parallel to the edge of this old cloud entity. The squall line of 4-5 September may have formed along the edge of a pool of cool downdraft air left behind by the old cluster.

## Large-scale flow in the vicinity of the squall-line system

The squall-line system on 4-5 September 1974 was associated with a synoptic-scale African Wave, of the type described by Carlson (1969a,b), Burpee (1972, 1974, 1975) and Reed et al. (1977). The position of the squall line determined from radar data discussed in Section 8 is shown in relation to wave categories analyzed by Reed et al. (1977) in Fig. 4. The winds in Fig. 4 were band-pass filtered to reduce the amplitudes of waves with periods shorter than 2 days and longer than 3-4 days by a factor of 2 or more. Waves with 3-5 day periods are almost fully retained. The position of the squall line between the upstream trough and downstream ridge of the wave (between wave categories 1 and 2 in Fig. 4) was typical of GATE squall lines (Payne and McGarry, 1977). Payne and McGarry found that

their squall lines typically propagated faster than the large-scale wave, but they tracked the squall lines only during their earlier stages. The squall line examined in the present study propagated slightly faster than the wave during its early stages, but later in its lifetime the squall line moved slower than the wave, and by 0600 on 5 September the squall line was located between wave categories 2 and 3.

Unfiltered winds, which depict the total airflow in the vicinity of the squall line, are shown in Fig. 5. These winds varied so greatly with height that four levels are included in Fig. 5 to depict the airflow completely. Continuous surface wind traces obtained aboard ships over which the squall line passed clearly showed the wind shift associated with the squall front (Sections 6 and 12). The disturbed portion of the wind field existed only in a very narrow region immediately behind the squall front and did not appear in the 6 h wind reports shown in Fig. 5. The analyses in Fig. 5, therefore, depict only the synoptic-scale flow in which the squall-line was embedded. The flow relative to the squall line, obtained by subtracting the squall-line propagation velocity from the observed wind, is shown

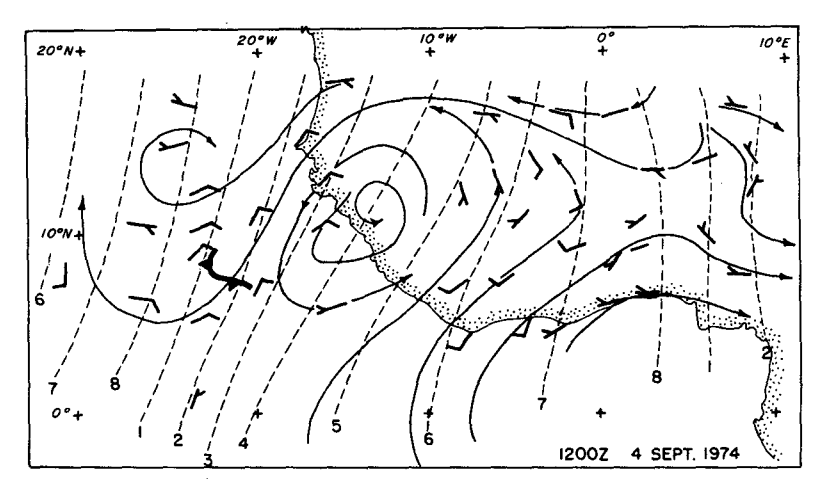


Fig. 4. Streamline analysis of band-pass filtered 700 mb winds for 1200 GMT 4 September 1974. Full wind barb is for 5 m s<sup>-1</sup>, half barb 2.5 m s<sup>-1</sup>. Dashed lines show wave phase categories determined by Reed *et al.* (1977). Front symbol indicates position of leading edge of squall line.

in Figs. 6a-6c for the three map times, corresponding, respectively, to Figs. 5a-5c.

The surface maps in Fig. 5 all show a confluence zone (the ITCZ) separating northwesterly winds to the north from southwesterly winds to the south. The prevailing westerly components of low-level winds over the GATE area are associated with the West African monsoon. At 1200 GMT 4 September (Fig. 5a), the developing squall line was north of the confluence zone moving through the region of surface northwesterlies. By 1800 (Fig. 5b) the mature squall line had moved southward relative to the confluence zone, so that it was located in the region of surface southwesterlies, and it remained there through its later stages (Fig. 5c). The 850 mb winds in the vicinity of the squall line tended to be northerly through the period shown in Fig. 5, except for the shift to westerlies just ahead of the squall line at 1800.

Since the surface and 850 mb winds were always either parallel to the squall line or blowing with a component opposite to the direction of squall-line propagation, the relative flow centered on the squall line (Fig. 6) at these low levels was from ahead of the squall line at each of the three observation times.

The strongest winds in the squall line's environment were the northeasterlies observed at the 700 mb level (Fig. 5) between the upstream trough and downstream ridge of the African wave. The northeasterly flow between the trough and ridge was unperturbed until the later stages of the squall line's life time. By 0000 on 5 September, however, a small-scale cyclonic circulation had formed at 700 mb in the trailing portion of the squall line system.

The 700 mb flow relative to the squall line is different at each of the times indicated in Fig. 6. At 1200 on 4 September (Fig. 6a), the relative flow at 700 mb is almost zero. The 700 mb winds reported at 1200

(Fig. 5a) were all from ships located ahead of the line. whereas at 1800, when wind measurements to the rear of the squall line were obtained (Fig. 5b), the relative flow at 700 mb (Fig. 6b) was quite strongly from the rear of the line. The weak relative 700 mb flow at 1200 (Fig. 6a) was therefore more representative of the region just ahead of the squall line during its early stages, and the 700 mb relative flow from the rear of the line (Fig. 6b) was more representative of the area immediately behind the line during the middle stages of the squall line's lifetime. This 700 mb inflow from the rear of the mature squall line is similar to that observed in other squall lines (Zipser, 1969; Obasi, 1974; Betts et al., 1976) and, as pointed out by Zipser (1977), may be the result of middle-level convergence induced by the squall-line circulation. The 700 mb relative flow at 0000 on 5 September, appears from Fig. 6c to have been from ahead of the squall line, but, as indicated by the erratic reports in Fig. 5c, the 700 mb winds appeared to be somewhat less reliable at this time.

The 500 mb flow in the vicinity of the squall line throughout its lifetime was similar to that at 700 mb, except that the reported speeds were somewhat lower at 500 mb. At the 200 mb level, evidence of divergence is seen at all three times in Fig. 5. At 1200 on 4 September, the 200 mb wind speeds were greater downstream and lower upstream from the squall-line system (Fig. 5a). At 1800, evidence of anticyclonic circulation is seen directly over the squall-line system (Fig. 5b), and by 0000 on 5 September the 200 mb flow field was highly perturbed with a diffluent source directly over the squall line system (Fig. 5c). These patterns indicate that the 200 mb (or 12.5 km) level was an important level of outflow for the squall-line system. The diffluent source observed at 200 mb at 0000 on 5 September developed simultaneously with the small-scale cyclonic circulation at 700 mb seen in Fig. 5c.

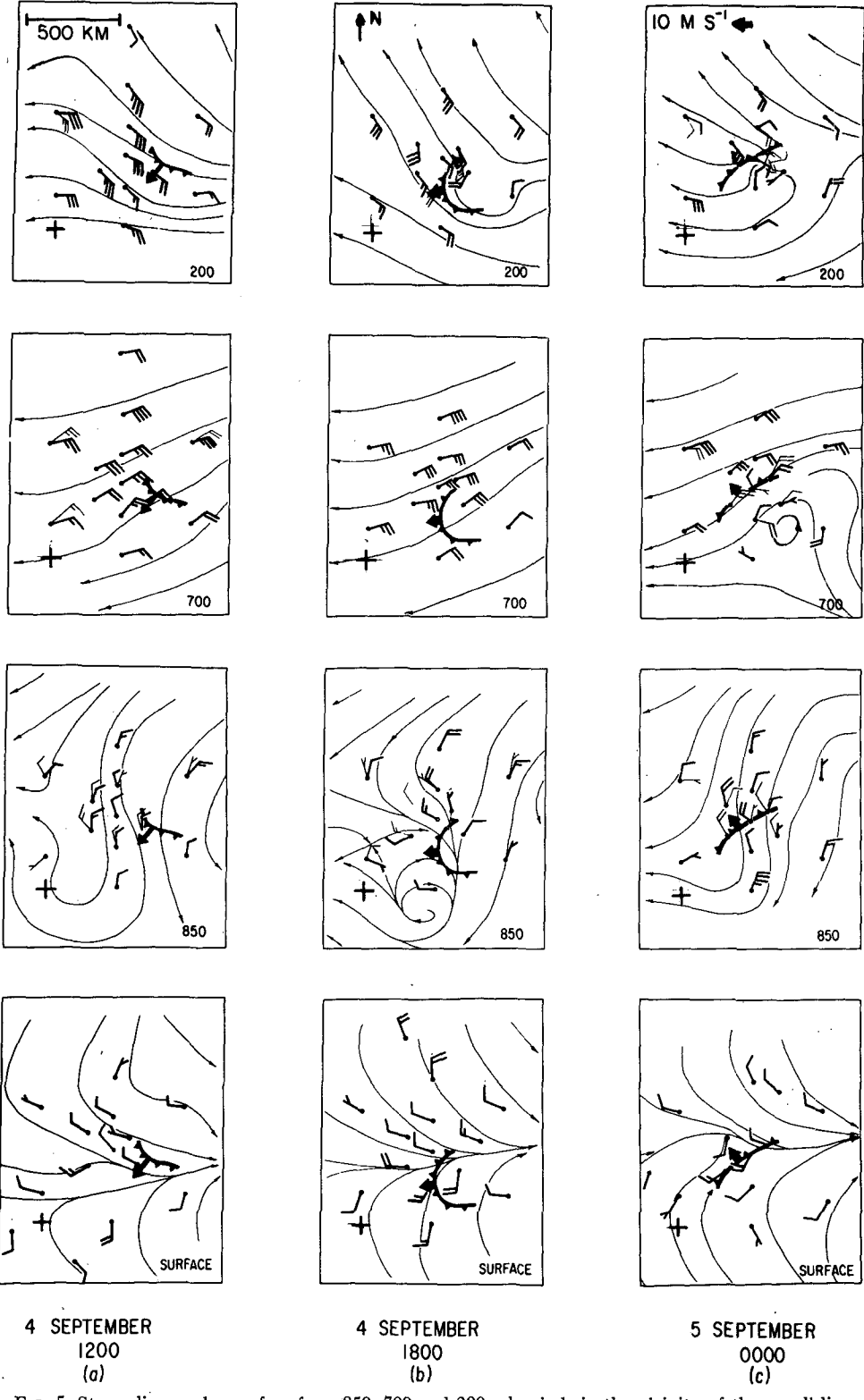
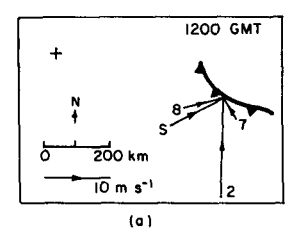
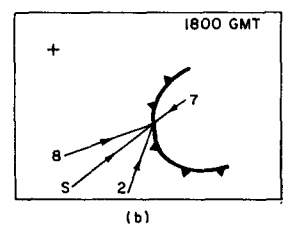


Fig. 5. Streamline analyses of surface, 850, 700 and 200 mb winds in the vicinity of the squall line. Frontal symbol indicates positions of leading edge of squall line. Heavy arrow indicates squall line velocity. Heavy wind barbs are for "Quick Look Data Set" winds. Light barbs are for "Nationally Processed and Validated" winds. Full barb is for 5 m s<sup>-1</sup>, half barb 2.5 m s<sup>-1</sup>. In cases where heavy and light barbs disagree by more than 10° or 5 m s<sup>-1</sup>, both barbs are plotted. Times are GMT. All boxes cover same geographical area. Cross is at 5°N, 27°W.





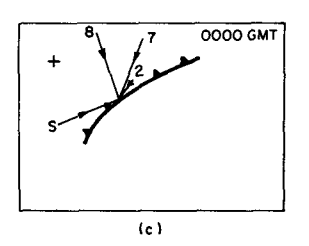


Fig. 6. Winds relative to squall line plotted as vectors for surface (S), 850 mb (8), 700 mb (7) and 200 mb (2) levels. Frontal symbol indicates leading edge of squall line. Cross is at 9°N, 26°W.

Fig. 7 was derived from Oceanographer wind soundings launched before and after the squall line passed over the ship on 4 September. The sounding obtained at 1200 GMT 4 September, just before the squall-line passage, showed inflow toward the leading edge of the squall line at all levels, with strong inflows at upper and lower levels and weaker inflows at middle levels. The 1800 sounding, obtained near the rear edge of the squall-line system, showed outflow at upper and lower levels, with inflow from the rear between 800 and 470 mb. These wind profiles are consistent with the relative flow patterns indicated in Fig. 6 and are quite similar in appearance to the composited relative wind profiles of Obasi (1974) and Betts et al. (1976).

The relative airflow pattern deduced in this section has been incorporated into the schematic summary of squall-line structure (Fig. 2). Air approaches from ahead of the squall-line system at both lower and upper levels and from the rear of the system in the midtroposphere. Air departs from the rear of the storm at both lower and upper levels. The airflow relative to squall-line elements is considered further in Section 13.

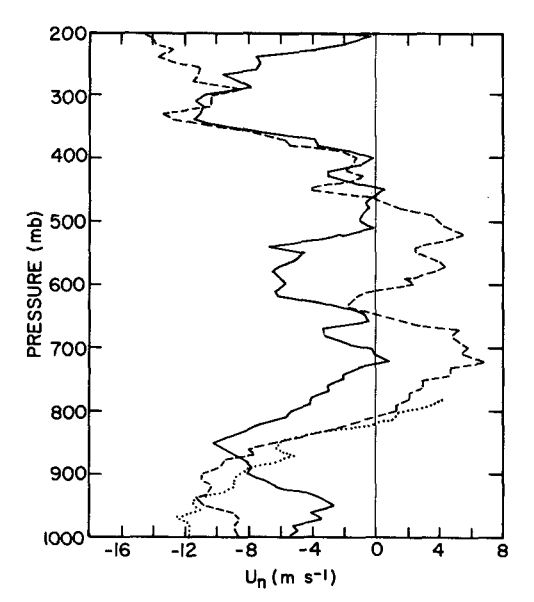


Fig. 7. Relative wind component normal to the squall line shown by *Oceanographer* soundings at 1200 (solid), 1500 (dotted) and 1800 (dashed) GMT 4 September 1974.

# 6. Squall-line circulation features deduced from wind and thermodynamic data

The wet-bulb potential temperature  $(\theta_w)$  and water vapor mixing ratio (q) profiles in Figs. 8 and 9 were obtained at the same times as the relative wind profiles in Fig. 7 and indicate the overturning of the atmosphere accomplished by the squall-line system. Below the 800 mb level, the values of both  $\theta_w$  and q decreased during the passage of the squall-line system between 1200 and 1800 on 4 September, while above the 500 mb level they increased. These layers corresponded, respectively, to the lower and upper level outflow layers at the rear of the squall line seen in the 1800 GMT relative wind profile in Fig. 7 and illustrated in Fig. 2.

The lowering of  $\theta_w$  and q in the lower level outflow layer at 1800 indicates that dry, mid-tropospheric, low- $\theta_w$  air, which entered the system from both front and rear (between 800 and 470 mb in Fig. 7), was transported downward into the lower troposphere within the squall-line system and exited from the rear of the

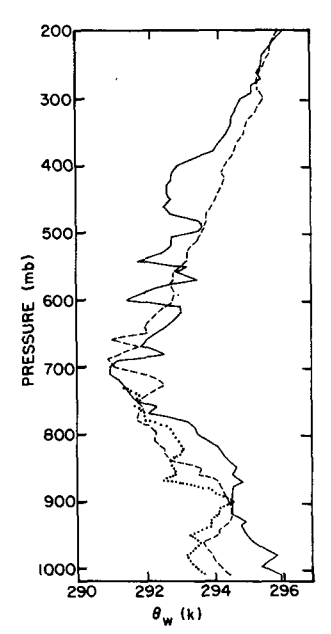


Fig. 8. Wet-bulb potential temperature  $(\theta_w)$  shown by Ocean-ographer soundings at 1200 (solid), 1500 (dotted) and 1800 (dashed) GMT 4 September 1974.

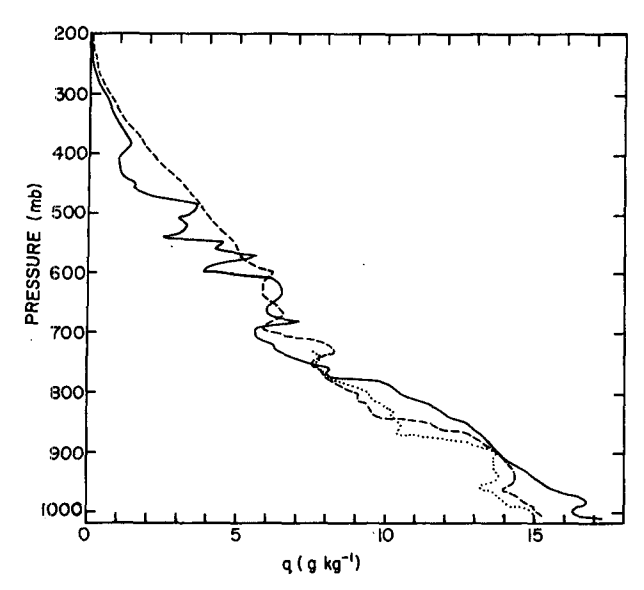


Fig. 9. Water vapor mixing ratio (q) shown by Oceanographer soundings at 1200 (solid), 1500 (dotted) and 1800 (dashed) GMT 4 September 1974.

system at low levels, as indicated in Fig. 2. The high values of  $\theta_w$  and q in the upper level outflow layer, seen after the squall-line passage at 1800, indicate that

boundary-layer air, which entered ahead of the squall line (Fig. 7), rose within the squall-line system and exited from the system as outflow from its trailing edge aloft.

This pattern of overturning is similar to the mean airflow patterns deduced by Obasi (1974) and Betts et al. (1976) by compositing soundings obtained in the vicinity of tropical squall lines.

The horizontal extent of the downdraft region of the squall-line system is indicated by the vertical time section in Fig. 10, which shows the field of  $\theta_w$  before, during and after the passage of the squall-line system over the Oceanographer. Before the passage of the leading edge of the squall line, the troposphere had a structure typical of the tropics, with high values of  $\theta_w$  near the surface and aloft and a pronounced minimum of  $\theta_w$  between 600 and 700 mb. However, immediately after the passage of the leading edge of the squall-line system, the field of  $\theta_w$  changed. Low- $\theta_w$  air replaced the high- $\theta_w$  air at low levels for the entire period that the squall-line system was overhead (1320-2100 in Fig. 10). Thus, almost the entire horizontal area covered by the squall-line system was characterized by downdrafts (both convective and mesoscale) extending from the middle into the lower troposphere (Fig. 2).

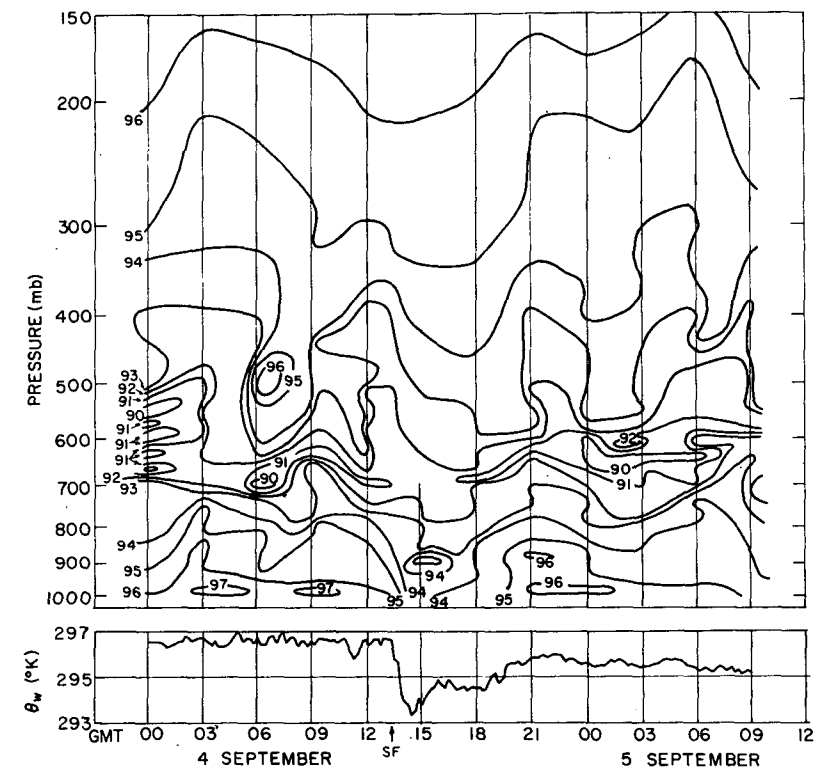


Fig. 10. Vertical-time section of wet-bulb potential temperature  $(\theta_w)$  constructed from Oceanographer soundings (indicated by vertical lines). Note that 1500 GMT sounding was terminated at 700 mb. Isotherms of  $\theta_w$  are labeled in kelvins with leading 2 omitted. Lower part of diagram is the surface trace of  $\theta_w$  constructed from 10 min average values measured on board the Oceanographer. SF indicates time of squall front passage.

The width of this downdraft region was about 200 km according to a time-to-space conversion based on the squall line's observed motion over the ship. After the passage of the back edge of the squall-line system, the troposphere eventually returned to the structure it had ahead of the squall-line system (Fig. 10, after 2100).

Figs. 11–13 show the influence of the downdrafts on the temperature, relative humidity and wind fields. In Fig. 11, it can be seen that the downdraft air (present between 1320 and 2100) was characterized by low temperatures which were evidently produced by the evaporation of hydrometeors when relatively dry midtropospheric air was entrained into the downdrafts. This evaporation also apparently led to the rather high relative humidities of the downdraft air evident between 1320 and 2100 in Fig. 12. However, the surface traces in Fig. 12 indicate that the downdraft air reaching the sea surface, in spite of its high relative humidity, was not quite saturated and that the mixing ratio of water vapor at low levels was actually much lower in the downdraft region than in the region ahead of the squall line.

In the wind field cross section shown in Fig. 13, winds with uncertainties (computed by Acheson,

1976) > 3 m s<sup>-1</sup> have been deleted and winds with uncertainties between 1 and 3 m s<sup>-1</sup> have been noted by an asterisk. The winds shown in Fig. 12 do not seem unreasonably noisy for qualitative analysis. During the period that the squall-line system was over the ship. large wind speeds, characteristic of the middle troposphere in the environment of the disturbance, appeared to extend downward into the low troposphere in the region influenced by squall-line downdrafts (1320-2100 in Fig. 13). The 3 min averaged surface winds reached 11 m s<sup>-1</sup> just behind the squall front (values in lower part of Fig. 13 are 10 min averages). These results suggest that downward advection of horizontal momentum or generation of horizontal momentum by horizontal pressure gradients existed within the downdrafts. However, uncertainty of the 900-750 mb level winds reported at 1500 in Fig. 13 makes this conclusion rather tentative.

## 7. Boundary-layer structure

According to Mandics and Hall (1976), acoustic sounder echoes during GATE were produced primarily by boundary-layer convective plumes, small convec-

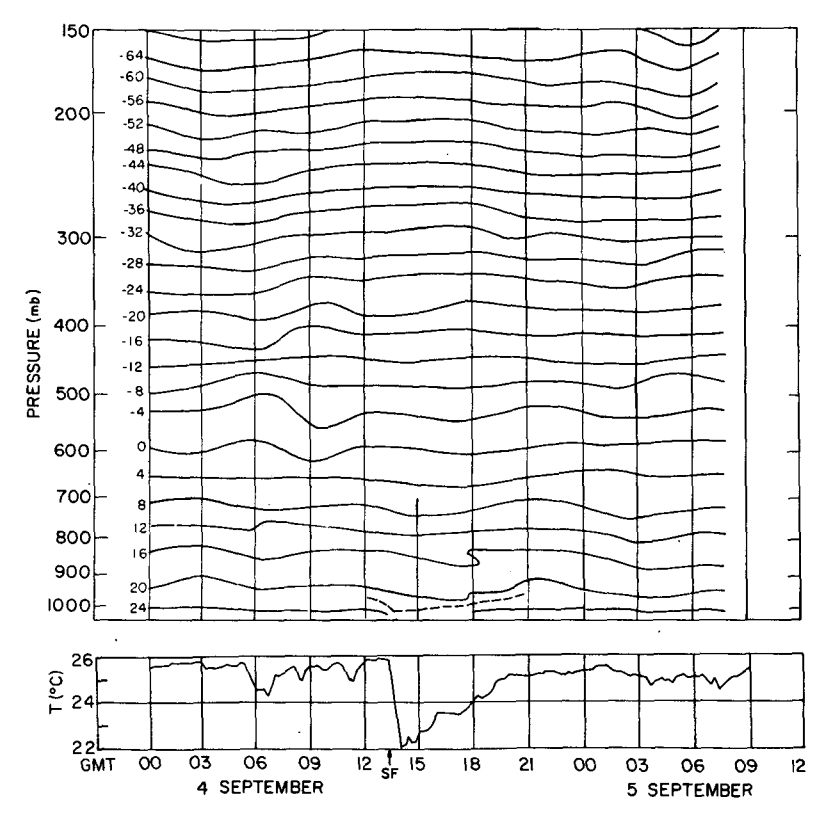


FIG. 11. Vertical-time section of temperature (T) constructed from Oceanographer soundings (indicated by vertical lines). Note that 1500 GMT sounding was terminated at 700 mb. Isotherms are labeled in °C. Dashed isotherm is for 22°C. Lower part of diagram is the surface trace of T constructed from 10 min average values measured on board the Oceanographer. SF indicates time of squall front passage.

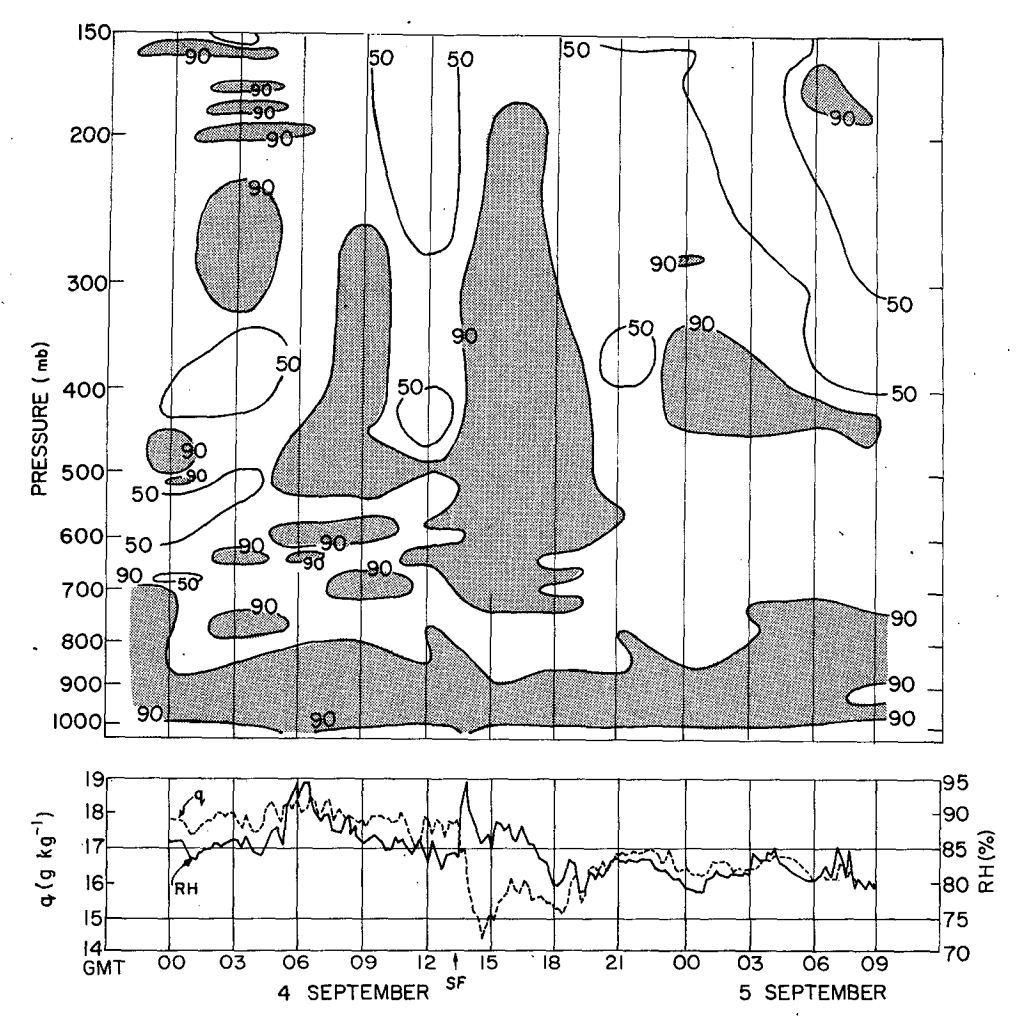


Fig. 12. Vertical-time section of relative humidity (RH) constructed from *Oceanographer* soundings (indicated by dashed lines). Note that 1500 GMT sounding was terminated at 700 mb. Contours of RH are labelled in percent with regions of RH>90% shaded. Lower part of diagram contains the surface traces of RH and mixing ratio q constructed from 10 min average values measured on board the *Oceanographer*. SF indicates time of squall front passage.

tive clouds and stable layers. Examples of all three of these phenomena can be seen in the Oceanographer acoustic sounder record for 4-5 September 1974, shown in Fig. 14. First, in the period prior to the onset of precipitation from the squall-line system at 1320 on 4 September echoes from turbulent convective plumes carrying heat and moisture upward from the warm sea surface are evident in the lowest 200 m of the boundary layer. These plume echoes are the vertically oriented spikes of high acoustic reflectivity seen emanating from the bottom of the acoustic sounder record. Echo spikes with bases at about 300 m appeared intermittently above the layer containing the surfacebased plumes during the period 0900-1320 and were apparently associated with low-level cumulus or stratocumulus clouds. These small cloud echoes seen during the period preceding the onset of rain from the squall-line system, are called "hummock" echoes by Mandics and Hall.

The sensible heat flux and evaporation from the ocean surface were computed by the bulk aerodynamic method (Roll, 1965, p. 251) from Oceanographer surface measurements (Fig. 14). For the period prior to the squall line's passage at 1320 on 4 September, these calculations confirm that mixing in the layer containing the turbulent plumes seen in the acoustic sounder data were transporting energy upward at a rate of about 5–10 W m<sup>-2</sup> and the radiosonde data for 0900 and 1200 (Fig. 14) show a well-mixed conditionally unstable boundary layer with potential temperature gradually increasing and mixing ratio decreasing with height.

Immediately following the squall-line passage at 1326, the sensible heat flux increased from about 5 to 20 W m<sup>-2</sup>, as the surface layer responded to the intrusion of cold downdraft air coming into contact the warm ocean surface (Fig. 11). The sounding for 1500 in Fig. 14 shows the extreme stability of the air between 1000 and 975 mb which apparently prevented turbulent

mixing in the superadiabatic layer below the 1000 mb level from penetrating above a height of about 100 m.

The surface evaporation rate followed generally the same patterns as the sensible heat flux (Fig. 14), except that the evaporation rate changed less dramatically with the passage of the squall front. The peak evaporation rate reached during the passage of the squall-line system was 8 mm day<sup>-1</sup>. This value was observed around 1800 which was the period of strongest sustained surface winds associated with the system (lower part of Fig. 13).

When the acoustic sounder was re-started after the long period of rainfall from the squall-line system, it showed a continuous, dark, undulating streak of echo located between the 200 and 400 m levels. This is an example of an echo produced by a stable layer. This prominent stable layer apparently formed the upper boundary of the layer of cold convective-scale downdraft air flowing out from the rear of the squall-line system (Fig. 2). As this cold air moved over the warm ocean, particularly strong turbulent mixing resulted below the stable layer in order to restore a thermo-

dynamic balance between the sea surface and the overriding air. The pattern of plume echoes seen immediately after 1820 was, therefore, denser than before the squall line's passage at 1320, and the computed heat fluxes were correspondingly higher. The radiosonde data in Fig. 14 show that the mean potential temperature in the mixed region below the stable layer increased from 1500 to 1800 and, again, from 1800 to 2100, as the heat flux from the sea surface gradually warmed the layer of downdraft air.

It is impressive that the downdraft outflow layer, which appears so prominantly in the acoustic sounder data was maintained over the sea surface for more than 9 h. A partial explanation for the persistence of this feature may be that the downdraft layer in contact with the sea surface emanated from intense convective-scale downdrafts at the leading edge of the squall-line system. When this air spread over the sea surface behind the squall line, it flowed under the broad mesoscale region of subsidence in the middle to lower troposphere below the large trailing upper level anvil cloud (Fig. 2). This large-scale sinking motion probably helped to

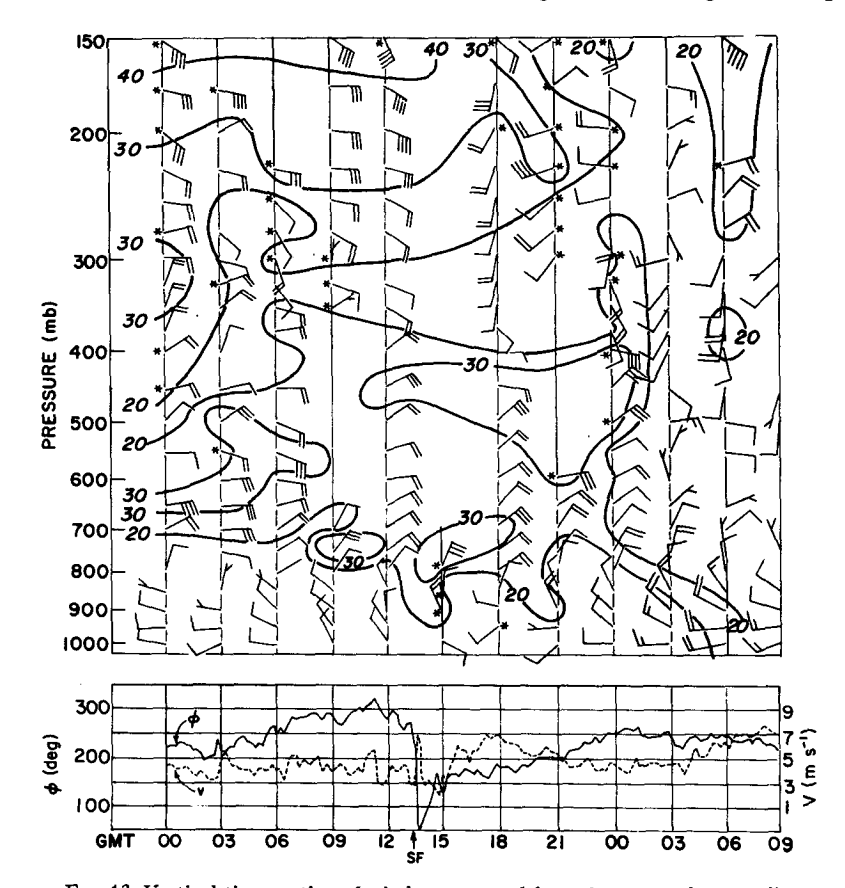
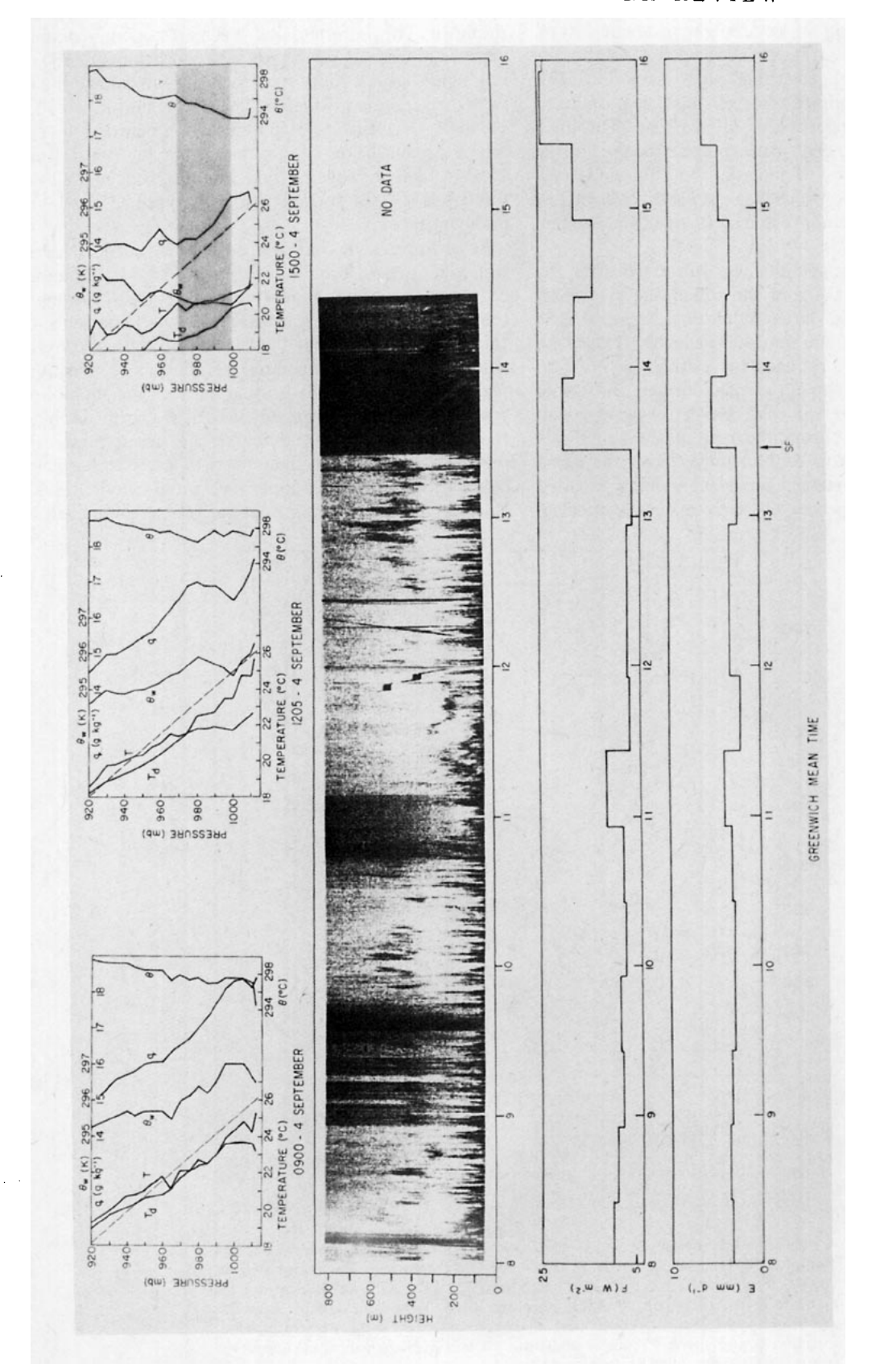


Fig. 13. Vertical-time section of wind constructed from Oceanographer soundings (indicated by vertical lines). Note that 1500 GMT sounding was terminated at 700 mb. Full wind barb is for 5 m s<sup>-1</sup>, half barb 2.5 m s<sup>-1</sup>. Asterisks indicate winds accurate to within 1-3 m s<sup>-1</sup>. More uncertain winds have been deleted. Isotachs are in units of 0.5 m s<sup>-1</sup>. Lower part of diagram contains surface traces of wind direction  $\phi$  and speed V constructed from 10 min average values measured on board the Oceanographer. SF indicates time of squall front passage.



q = mixing ratio,  $\theta$  = potential temperature. Dashed line is dry adiabat for  $\theta$  = 25°C. Note that 920 mb level is ~800 m above the sea surface in each sounding. Shading shows stable layer referred to in text. Photograph in middle part of figure shows acoustic sounder data obtained on board Oceanographer on 4 September 1974. Black echoes extending from top to bottom of chart are from precipitation. Rectangular echoes at 1150-1200, 1845-1940 and 2015 GMT are from tethered balloon instruments flown from Fig. 14. Boundary-layer data. Upper part of figure contains radiosonde data from Oceanographer.  $T_d$ -dew point, T-temperature,  $\theta_w$ -wet-bulb potential temperature, the Oceanographer. Spikey echoes emanating from bottom of chart are from turbulent plumes. Intermittent echoes between 300 and 600 m levels prior to 1325 are cloud or "hummock" echoes. Continuous layer of echo after 1815 is from stable layer. Lower part of figure shows sensible heat flux F and evaporation E computed by bulk aerodynamic method. SF indicates time of squall front passage.

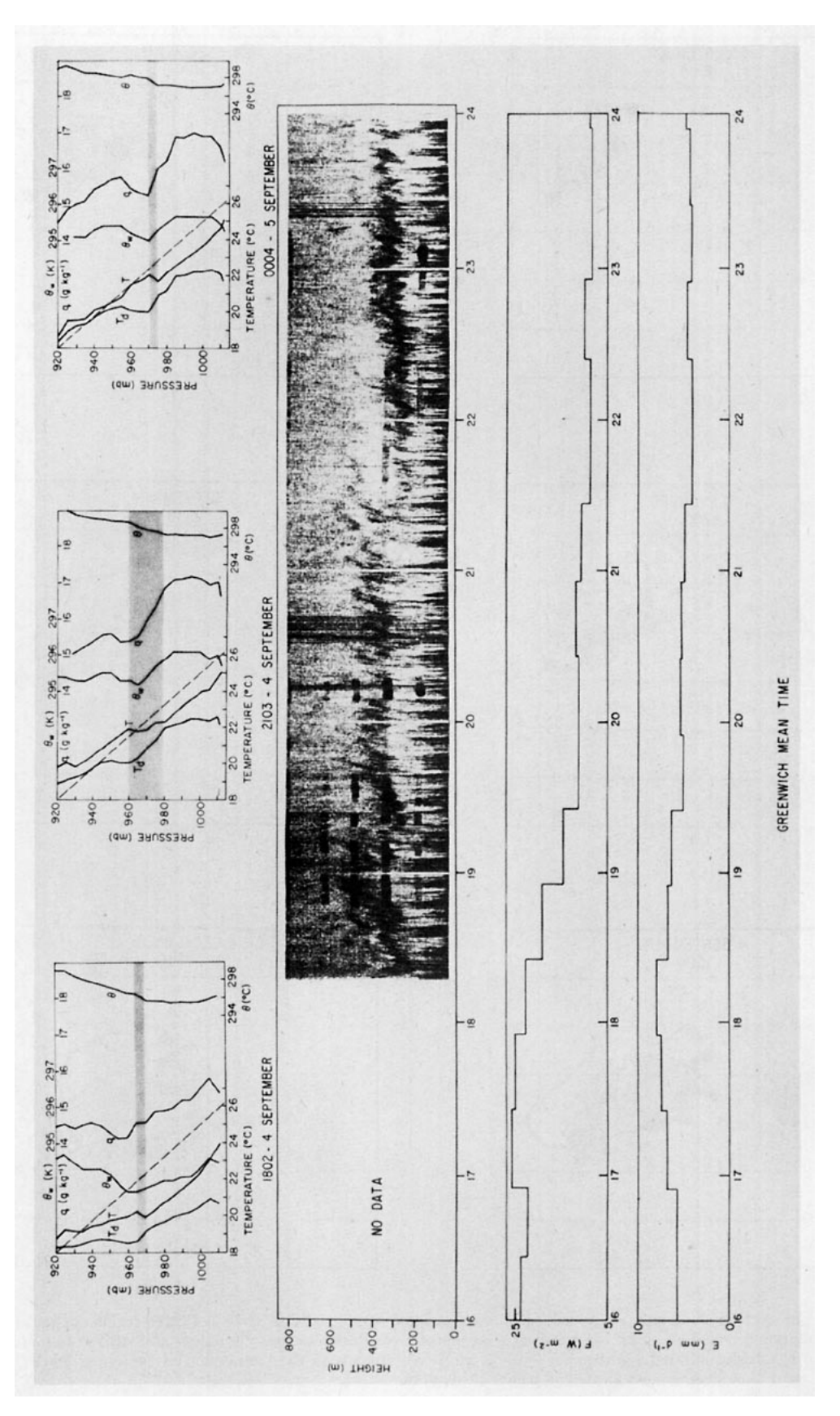


FIG. 14 continued.

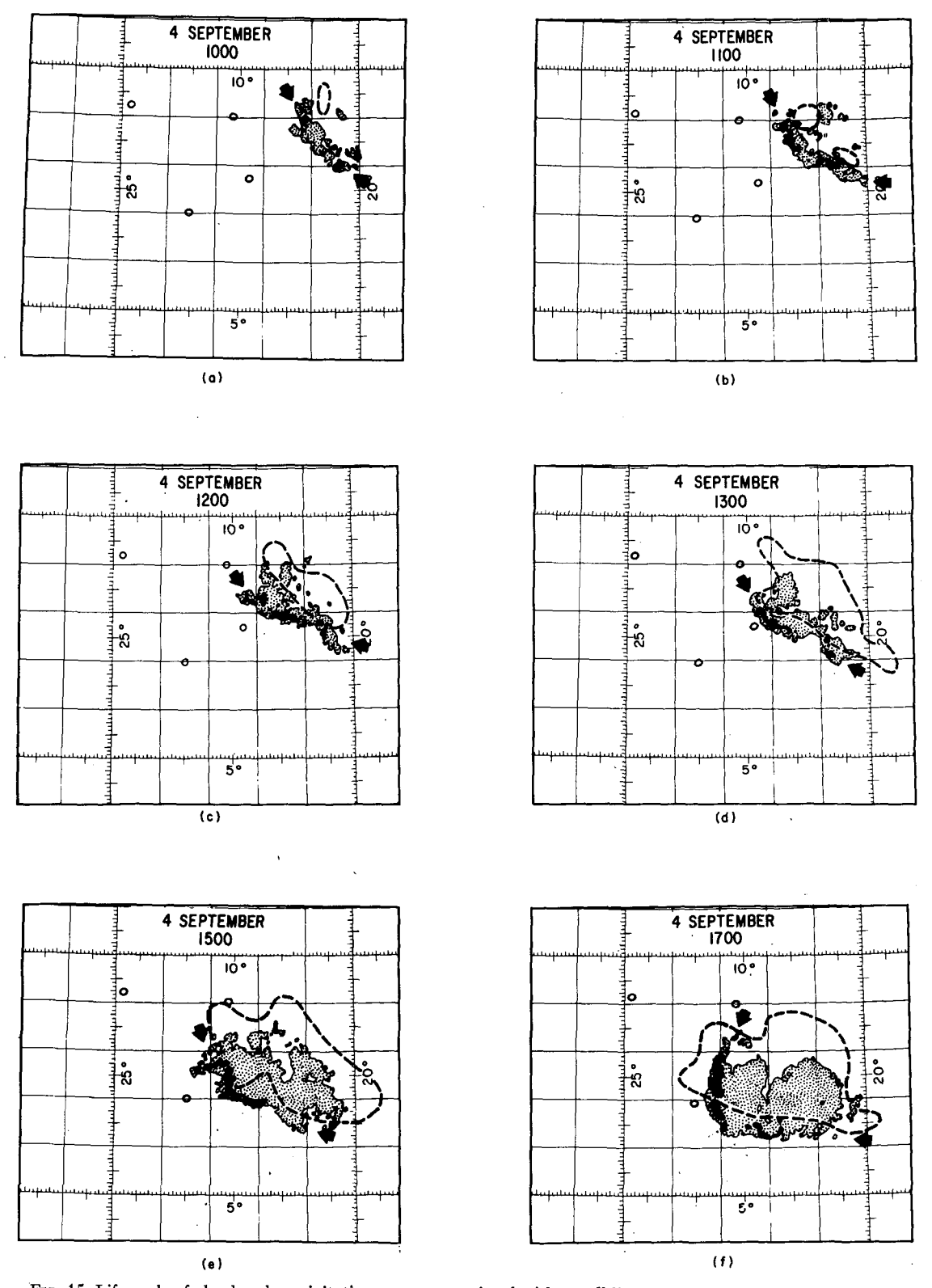


Fig. 15. Life cycle of cloud and precipitation pattern associated with squall-line system. Dotted region encloses low-level precipitation detected by radar. Black indicates regions of precipitation intensity in excess of 38 dBZ or 14 mm  $h^{-1}$ . Dashed line is satellite infrared isotherm for  $-47^{\circ}$ C which corresponds to the intersection of the upper level cloud shield with the 11 km level. Arrows locate end points of squall line.

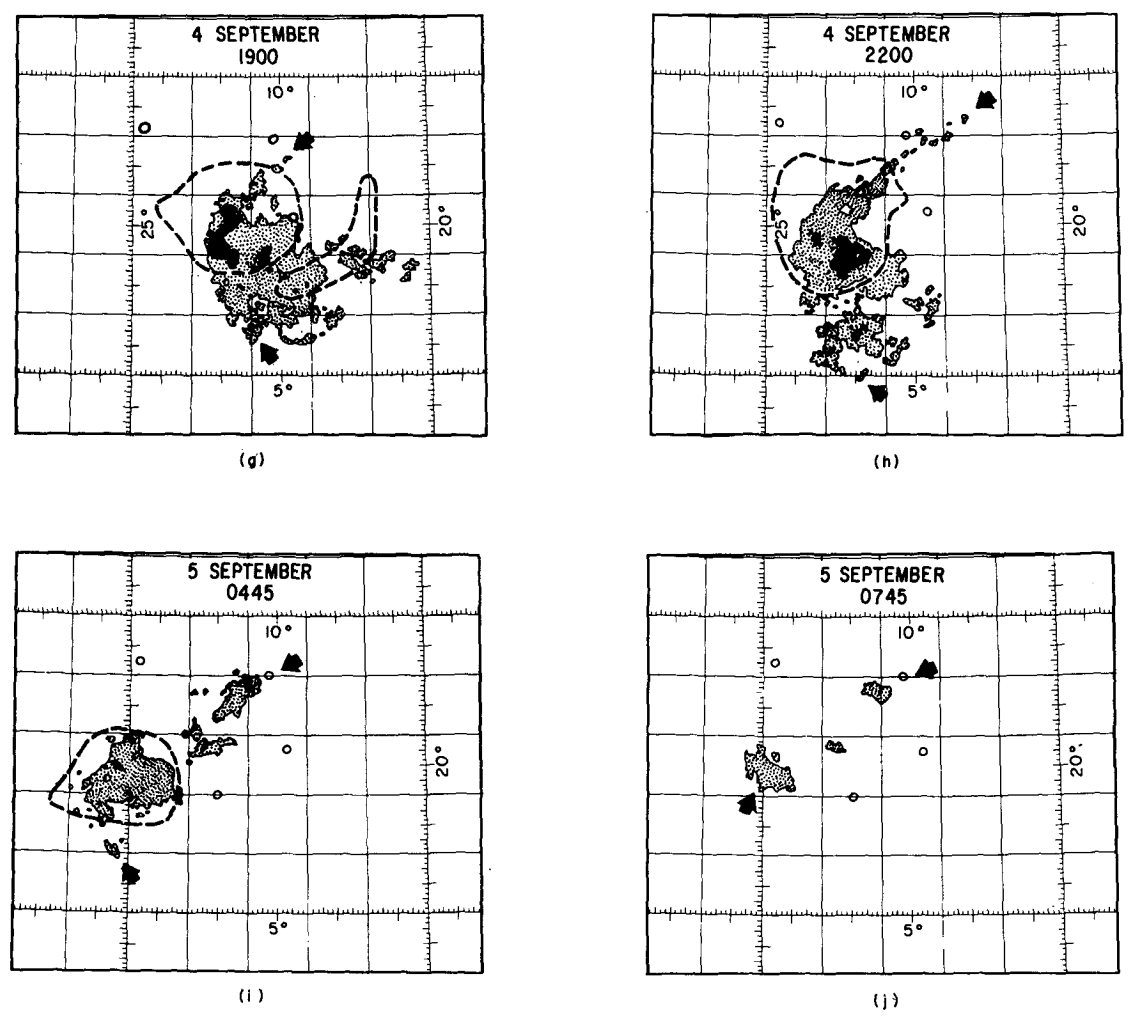


Fig. 15 continued.

maintain the stable layer. A similar structure has been suggested by Zipser (1977).

# 8. Development of the cloud and precipitation structure of the squall-line system

In Fig. 15, quantitative radar reflectivity patterns have been combined with infrared satellite imagery to show an overall history of the GATE 4–5 September squall-line system. The radar reflectivity patterns show the low-altitude precipitation pattern, while the satellite data show the upper level clouds associated with the system.

The radar patterns in Fig. 15 are analyses of maps showing the average radar reflectivity in 4 km×4 km horizontal grid squares covering the entire GATE radar area (Fig. 1). Base-level elevation angle data were used to indicate the low-altitude precipitation pattern in all of the grid squares except those within 30 km of each of the four radar-equipped ships. In these regions close to the ships, data from higher tilt angles were used to

avoid sea clutter echoes at the base-level elevation angle (Hudlow, 1976a,b). In areas of overlapping radar coverage, the correct radar reflectivity in a particular grid space was assumed to be the one from the radar indicating the highest value for that square since the calibrated radar signals would not have overestimated the true intensity of a precipitation feature, but might have underestimated it as a result of signal attenuation or beam geometry.<sup>4</sup>

The dashed contour in Fig. 15 indicates the satellite infrared brightness value corresponding to a cloud top temperature of  $\sim -47^{\circ}\mathrm{C}$  (Lienesch, 1975) or an altitude of about 11 km. The clouds enclosed by the dashed contour include only those portions of the upper level cloud shield which extend above this level. Generally, the dashed line defines the boundary of the upper level

<sup>&</sup>lt;sup>4</sup> Measurements from the four GATE quantitative shipboard radars were intercompared using data obtained with the ships in both colocated and noncolocated positions and this information has been taken into account in the analysis.

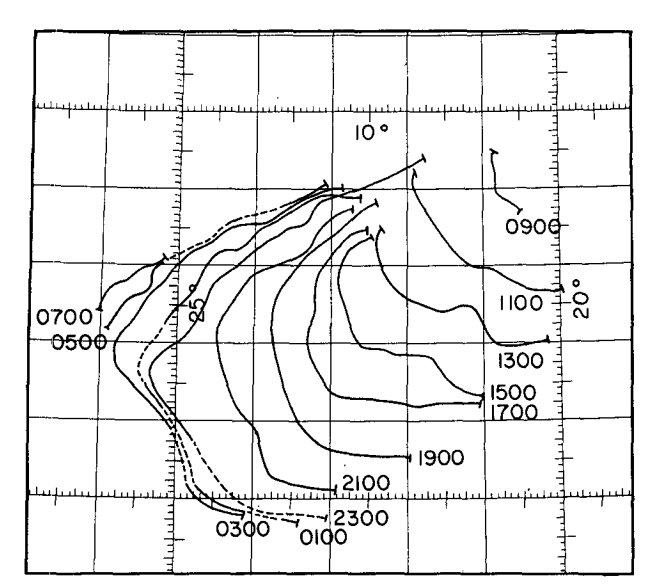


Fig. 16. Successive positions of the leading edge of the squall line. Times are GMT, beginning with 0900 on 4 September and ending with 0700 on 5 September 1974.

anvil cloud associated with the squall-line system (Fig. 2).

The squall line first appeared at about 0900 on 4 September 1974, and by 1000 it formed the welldefined line of echoes seen in Fig. 15a. This line was moving southwestward, toward the Oceanographer, at 12 m s<sup>-1</sup> [a typical speed for GATE squall lines (Houze, 1975) but an anomalously rapid rate for GATE echoes in general (Houze and Cheng, 1977). The upper level cloud associated with the squall line, evident as the two white dots in Fig. 3b, did not penetrate high enough to produce a dashed contour in Fig. 15 until 1100 when two patches of high-infrared brightness appeared above the line of radar echoes (Fig. 15b). These patches of high cloud quickly grew, merged and expanded, forming a single, large, high-level anvil cloud (Fig. 15c). This high anvil cloud trailed the southwestward-moving squall line, and the squall-line system thus began to resemble the schematic picture shown in Fig. 2.

The lag between the leading edges of the low-level radar echo formed by the squall line and the upper level anvil cloud (Figs. 15c and 15d) indicates that the squall-line system had a sloping front edge. This slope is discussed further in Section 11.

The anvil cloud continued to expand, nearly doubling its size between 1200 and 1300 (Figs. 15c and 15d). Patches of light rain falling from the anvil cloud behind the anvil cloud behind the squall line were beginning to appear at these times. By 1500 (Fig. 15e), the squall-line system had matured and bore its strongest resemblance to the idealized model in Fig. 2, with both the squall line itself and the extensive region of light rain falling from the trailing anvil cloud being fully developed features.

The echo pattern for 1700 (Fig. 15f) shows the

squall-line system near the peak of its overall intensity. (The variation of intensity of the squall-line system is discussed further in Section 16.) By this time, the central portion of the squall line had slowed to a speed of 7 m s<sup>-1</sup> and was moving west-southwestward toward the Researcher. As the squall line decelerated, the upper level air motion relative to the squall line (Fig. 6) changed, resulting in the northwestern portion of the anvil cloud flowing out ahead of the squall line, while the southeastern portion of the anvil remained to the rear of the squall line (Fig. 15f).

The squall-line system began to weaken after 1700. The anvil cloud was broken up by 1900 and was substantially reduced in size by 2200 (Figs. 15g and 15h). The entire squall line south of the *Researcher* was weak and spotty by 1900, and by 2200, the portion of the line immediately to the west of the *Researcher* had turned to stratiform precipitation.

At 1900, a new line of echoes was forming an extension of the squall line toward the northeast. By 2200, this northeastern extension of the line was well-developed, and a southeastern extension consisting of rather spotty echoes had also formed. These northeastern and southeastern extensions of the squall line did not appear to propagate as highly organized parts of the squall line. They were disconnected from the anvil precipitation zone which remained attached only to the central portion of the squall line.

After 2200 (Figs. 15h–15j), the central portion of the squall line and its attached region of anvil precipitation moved west-northwestward. By 0445 on 5 September the entire system was reduced in extent to the relatively small echo feature seen centered under the small anvil cloud in Fig. 15i. The system disappeared at about 0800. The region influenced by the squall-line system during its lifetime is shown in Fig. 16.

## Discrete nature of the squall line's structure and movement

When the radar data are examined with high temporal and spatial resolution, it is seen that the squall line consisted of discrete cores of convection, referred to here as *squall-line elements* or LE's.

In all, there were 21 LE's which could be tracked. Fig. 17 traces the life cycles of four typical LE's. At 0945 GMT (Fig. 17a) LE 2 was mature and located well within the squall line, while LE's 3, 4 and 5 were forming ahead of the line. By 1045 GMT (Fig. 17d), LE 2 was weakening at the rear of the squall line, while LE's 3 and 4 were at peak development and occupying the central portion of the squall line. LE 5 was still in a formative stage ahead of the squall line at this time. By 1145 GMT (Fig. 17g), LE 5 was taking shape rapidly, while LE 4 was weakening and becoming part of the trailing stratiform rain. LE 5 was best developed at 1245 GMT (Fig. 17i).

The sequence in Fig. 17 illustrates that during the

early history of the squall-line system, new LE's systematically formed on the leading edge or ahead of the existing squall line, while old LE's dissipated at the rear of the squall line. Remnants of the old LE's became part of the region of light rain falling from the trailing anvil cloud. This behavior of the LE's was similar to the cells in multicell hailstorms which begin as discrete clouds ahead of the storm and dissipate to the rear (Dennis et al., 1970; Browning et al., 1976).

The first appearance of LE 5 at such a large distance from the active squall line (Fig. 17a) indicates that the triggering mechanism for LE's may sometimes be independent of the downdraft spreading out from the existing squall line. One possibility is that LE 5, when it was initially observed far from the squall line, was a convective entity independent of the squall line until it interacted with the squall front. Then it suddenly intensified and began propagating as a major feature along the leading edge of the squall line. It is possible, however, that the squall line had an indirect effect on the wind field well ahead of the squall front, resulting in the formation of LE's such as LE 5, ahead of the existing squall line. Rosenthal (1977) has recently produced a discretely propagating squall line in a twodimensional model in which a new LE forms ahead of the squall line when the air column ahead of an active convective element is warmed by compensating downward motion and the surface pressure becomes sufficiently low to reverse the direction of low-level vertical

The systematic development of new LE's ahead of the squall line, followed by the subsequent incorporation of the LE's into the trailing anvil precipitation zone, was not so prevalent during later periods of the squall line's lifetime. By 2200 the squall line consisted of an active central portion, attached to the trailing anvil precipitation zone, and relatively spotty northeastern and southeastern extensions of the line (Figs. 15h and 18a). In the active central portion of the squall line, LE's continued to behave as they had earlier. For example, LE 20 appeared at 2230 (Fig. 18b) and remained through 2300 (Fig. 18c) and LE 21 appeared at 2330 (Fig. 18d). Generally, these LE's were smaller, weaker and shorter-lived than the ones which appeared earlier.

The echoes comprising the northeastern and south-eastern extensions of the squall line at 2200 (Fig. 15h) were isolated spots of convection, evidently forming along the edge of the broad mesoscale downdraft zone of cool air spreading out below the upper level anvil cloud, but did not become LE's themselves. They were not connected with, nor did they evolve into, a region of light stratiform precipitation. The spottiness of these echoes and their separation from the anvil cloud are reminiscent of Zipser's (1969) observation that during the dissipating stages of his squall-line system, the squall line degenerated into a line of cumulus

clouds which outran and became physically separated from the upper level anvil cloud. Hamilton and Archbold (1945) noted that when a squall line weakens, the ends often change from "a long continuous belt of thunderstorms" to "a line of heavy cloud." The northern and southern ends of the GATE 4–5 September squall line evidently followed this pattern.

### 10. Horizontal structure of squall-line elements

The low-level horizontal structure of the radar echo associated with each of the 21 observed LE's was followed in time with PPI patterns like those in Figs. 17 and 18. Each LE became elongated with its maximum length occurring at about the time that its highest surface rainfall rate was observed. For LE's 3 and 5, this occurred between 1045 and 1115 and at 1245, respectively (Fig. 17). The curved shape of LE 3, which was convex toward the leading edge of the squall line, was characteristic of several of the LE's suggesting that an LE contained a spreading downdraft of the scale of the LE itself. This conclusion is supported by the fact that the radius of curvature of LE 3 was considerably smaller than the radius of curvature of the squall line as a whole. Thus, it appears that the shape of the LE was determined by a convective-scale downdraft associated with the individual LE, while the position of the squall line as a whole, which consisted of several LE's, was determined by the leading edge of the much broader mesoscale downdraft associated with the trailing anvil cloud. These two scales of downdrafts are depicted in Fig. 2.

### 11. Vertical structure of the squall-line elements

The vertical structure of each LE was investigated by constructing RHI and CAPPI displays from the digitally recorded radar data described in Section 2. An RHI display is a vertical cross section showing the radar reflectivity pattern along a given azimuth, and CAPPI (Constant Altitude PPI) displays are horizontal cross sections showing the radar reflectivity pattern at selected altitudes. Figs. 19 and 20 show RHI and CAPPI displays extending through LE's 3 and 5. The azimuths along which the RHI's in Fig. 19 were constructed are indicated in Figs. 17 and 20.

Figs. 19 and 20 show that LE's 3 and 5 had a sloping structure in the vertical, suggesting that the updraft in each LE sloped as it rose over the downdraft. As the downdraft spread out at low levels, it maintained the updraft by generating low-level lifting at the squall front.

The updraft streamlines in Fig. 19c and Fig. 2 may not have been continuous, except in an average sense. The upward motion likely consisted of discrete bouyant bubbles released vertically at low levels in sequence controlled by the advancing edge of the convective-scale downdraft air. A temporary lapse in the release of

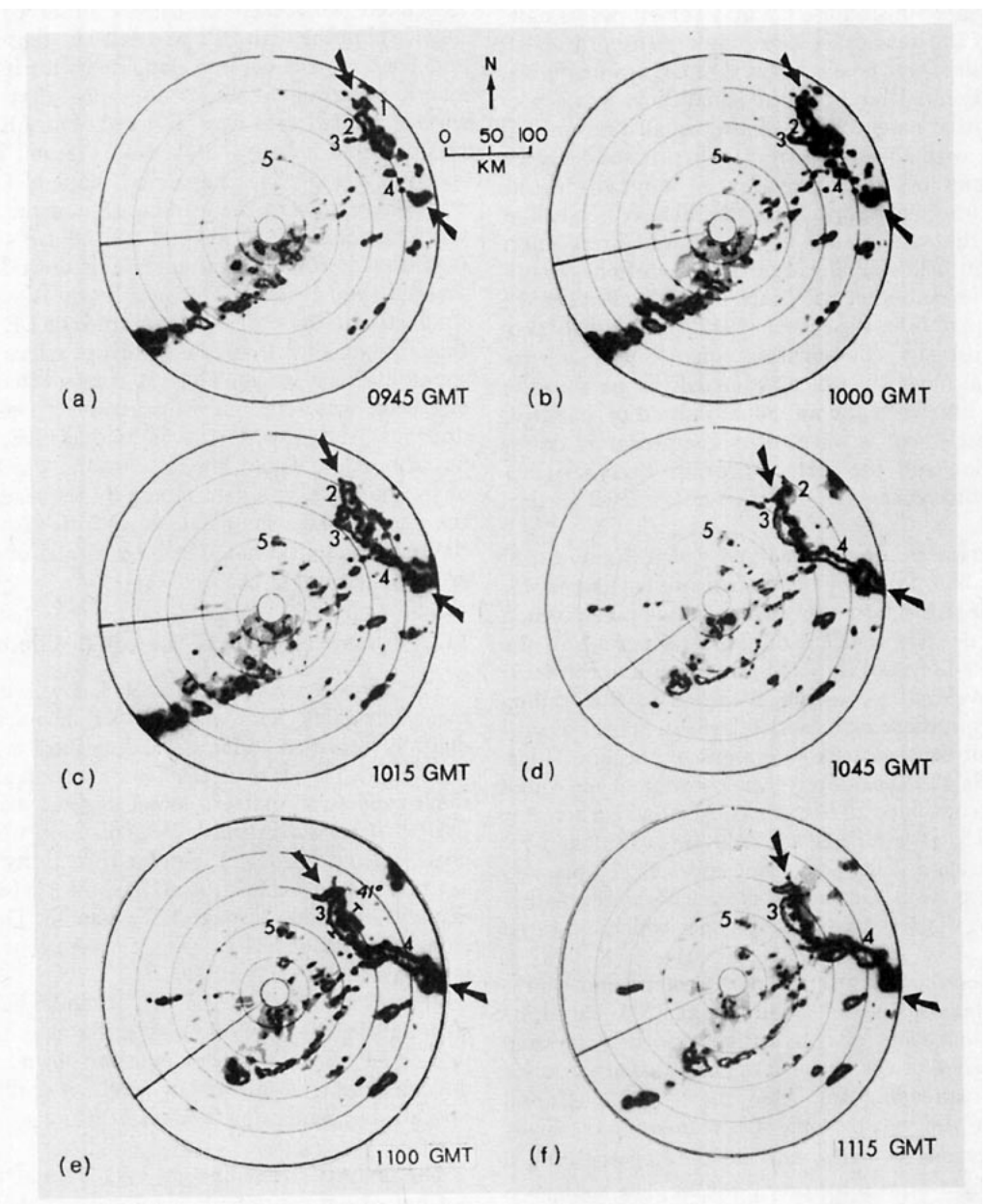
bubbles as the downdraft edge continued to advance might have resulted in an exaggerated or nearly discontinuous slope such as exhibited by LE 3 in Fig. 19a.

The downdraft indicated in Fig. 19c corresponds in scale to the convective-scale downdraft which produced the curvature of LE 3 noted in Section 10. It was sketched to coincide with the heaviest precipitation (highest radar reflectivity) in the LE since downdrafts of this scale normally occur in the zone of most concentrated precipitation in a cumulonimbus cloud and generally appear to be initiated by precipitation drag

(Brooks, 1922; Byers and Braham, 1949, pp. 24, 41–42; Ogura and Takahashi, 1971; Takeda, 1971; Wilhelmson, 1974; Miller and Pearce, 1974).

# 12. Weather events associated with the passage of a squall-line element

Surface weather events observed on board the Oceanographer on 4 September 1974 included a sudden shift in wind direction, an increase in wind speed, and dry and wet bulb temperature drops  $\sim 2$  min prior to the



4 mm h<sup>-1</sup> (black), 39 dBZ or 17 mm h<sup>-1</sup> (white), 47 dBZ or 74 mm h<sup>-1</sup> (gray). Radial line indicates ship heading (a 20° sector was blocked by the ship's superstructure in this direction). Azimuth lines (dashed) for cross sections shown in Figs. 15 and 25 are labeled in 17e, 17i and 17j.

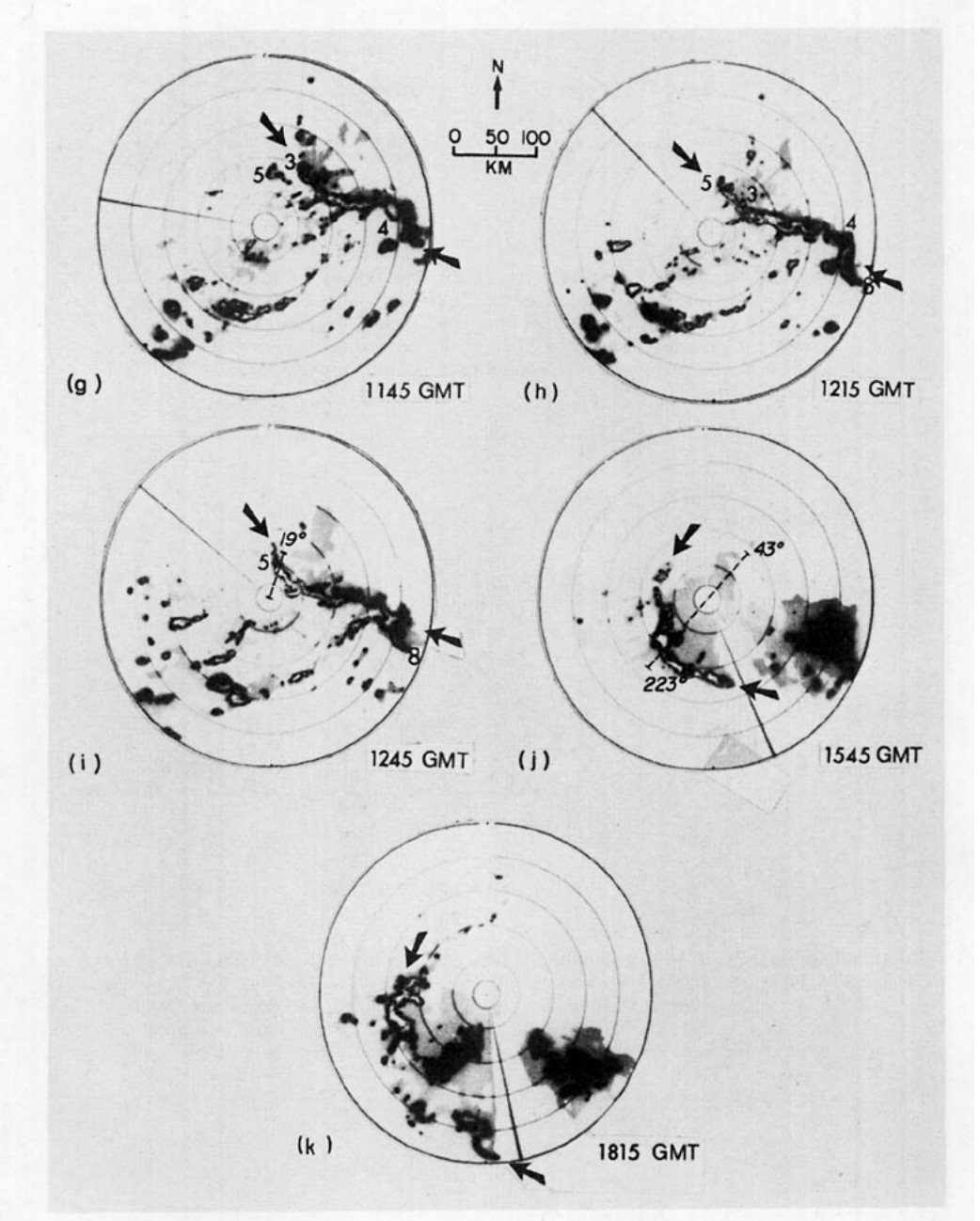


FIG. 17 continued.

onset of rain at the ship (Fig. 21; surface traces in Figs. 10-13). Immediately after the onset of rain, there was a pressure rise of  $\sim 1$  mb.

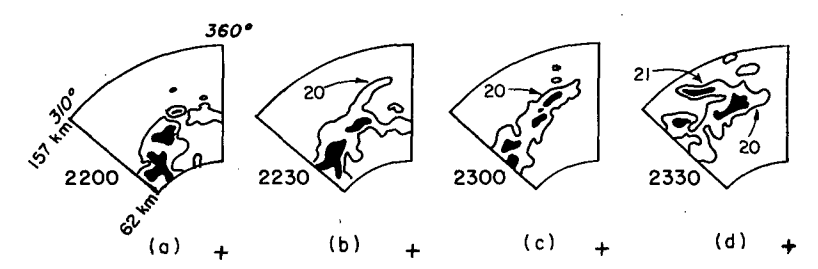
The sequence of all-sky camera pictures in Fig. 22 shows a low-level roll cloud (arcus) which passed over the ship just after the surface windshift. The cloud is further evidence that the wind shift marked the boundary of ascending and descending air currents (Humphreys, 1914).

The dramatic weather events observed at the Oceanographer were associated with LE 5 (Fig. 17). In general, the weather events accompanying squall-line

passages are associated with individual LE's, the convective units comprising the larger scale squall line.

# 13. Dynamics of squall-line elements

The small-scale squall-line elements contained within the GATE 4-5 September squall line appear to correspond to the tropical cumulonimbus cloud modeled by Moncrieff and Miller (1976). Their model developed a linear element about 12 km in length, and Moncrieff and Miller concluded that it corresponded to only a "segment" of an observed squall line of much greater



Frg. 18. Sequence of low-level echo patterns showing squall-line elements (LE's) 20 and 21 as they appeared on the *Researcher* radar's PPI on 4 September 1974. Range and azimuth (in degrees from true north) from radar site (indicated by cross) are indicated. Times are GMT. Outside echo contour is for about 28 dBZ or about 2 mm  $h^{-1}$  in rainfall rate, black area includes reflectivity values  $\geqslant$  36 dBZ or about 10 mm  $h^{-1}$ .

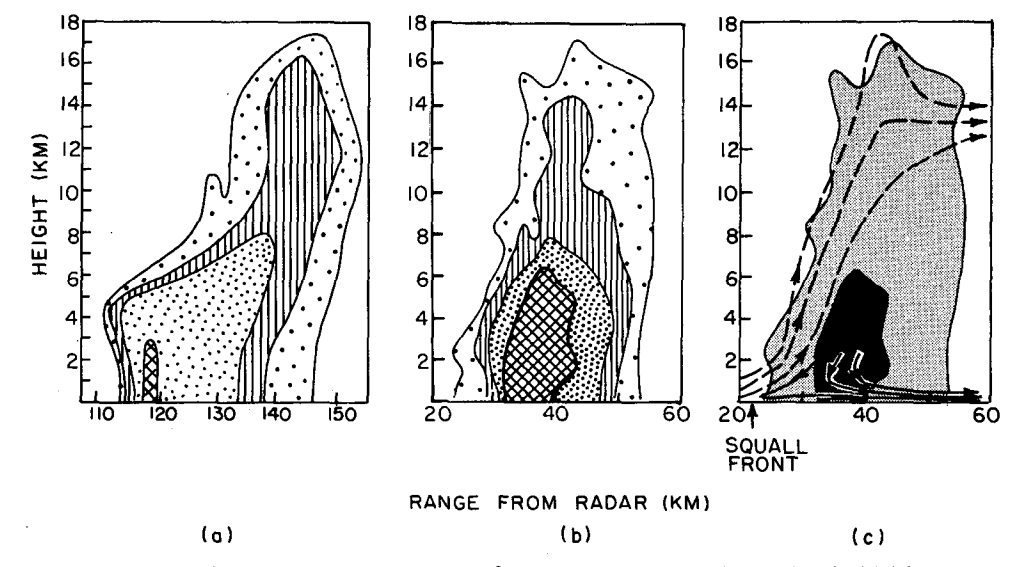


FIG. 19a. RHI through LE 3 along azimuth 41° from Oceanographer radar at 1100 GMT 4 September 1974 (see Fig. 17e); 19b. RHI along azimuth 19° through LE 5 at 1245 GMT 4 September 1974 (see Fig. 17i); 19c. suggested relative streamlines for updraft (dashed) and downdraft (solid) in LE 5. In (a) and (b), inside contours are for 23, 33 and 43 dBZ. Outside contour outlines weakest detectable echo. In (c), contours for 43 dBZ and weakest detectable echo are repeated from (b).

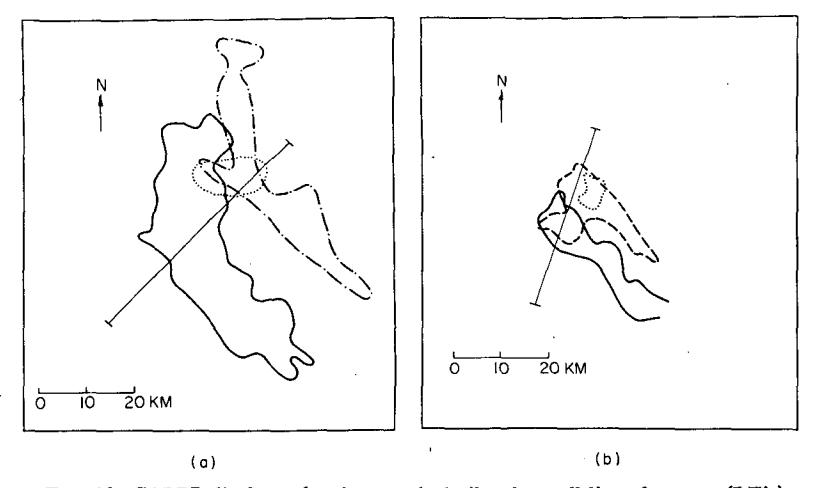


Fig. 20. CAPPI displays showing vertical tilt of squall-line elements (LE's): (a) LE 3 contours for 33 dBZ at the 2 km level (solid), 23 dBZ at 8 km (dash-dot) and 23 dBZ at 16 km (dotted); (b) LE 5 contours for 41 dBZ at the 0.5 km level (solid), 31 dBZ at 6 km (dash-dot) and 30 dBZ at 10 km (dotted). Bars across echo patterns locate cross sections shown in Fig. 19.

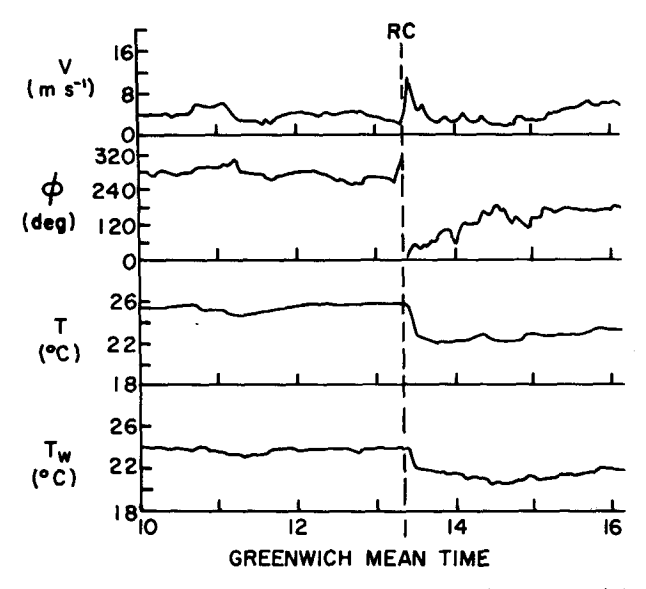


Fig. 21. Surface wind speed (V) and direction  $(\phi)$  and dry (T) and wet  $(T_w)$  bulb temperature at *Oceanographer* on 4 September 1974. RC is time that leading edge of roll cloud (Fig. 22) passed over ship just prior to onset of squall line precipitation. Time resolution of data is 3 min.

length. Their results suggest that the convective-scale downdraft air associated with a squall-line element actually originates ahead of the element, entering the downdraft region of the LE after flowing through gaps between updraft cores of LE's distributed along the leading edge of the squall line.

Since the squall line had a discrete rather than a continuous two-dimensional structure, it would have been possible for air from ahead of the line to flow between updrafts and become incorporated into convective-scale downdrafts on the trailing sides of LE's in a manner suggested by Moncrieff and Miller's model. To investigate whether the convective-scale downdrafts were actually fed from the front or rear, the winds relative to individual LE's were calculated, and are shown in Fig. 23. The motion vector for each LE is also included to make clear whether the relative winds are from the rear of the LE (had a component in the same direction as the element's motion) or from ahead of the element (had a component opposite to the element's motion vector. For LE's 3 and 5 (Figs. 17 and 19-22), the relative winds in Fig. 23 indicate that if the downdraft air originated near the 850 mb level or well above

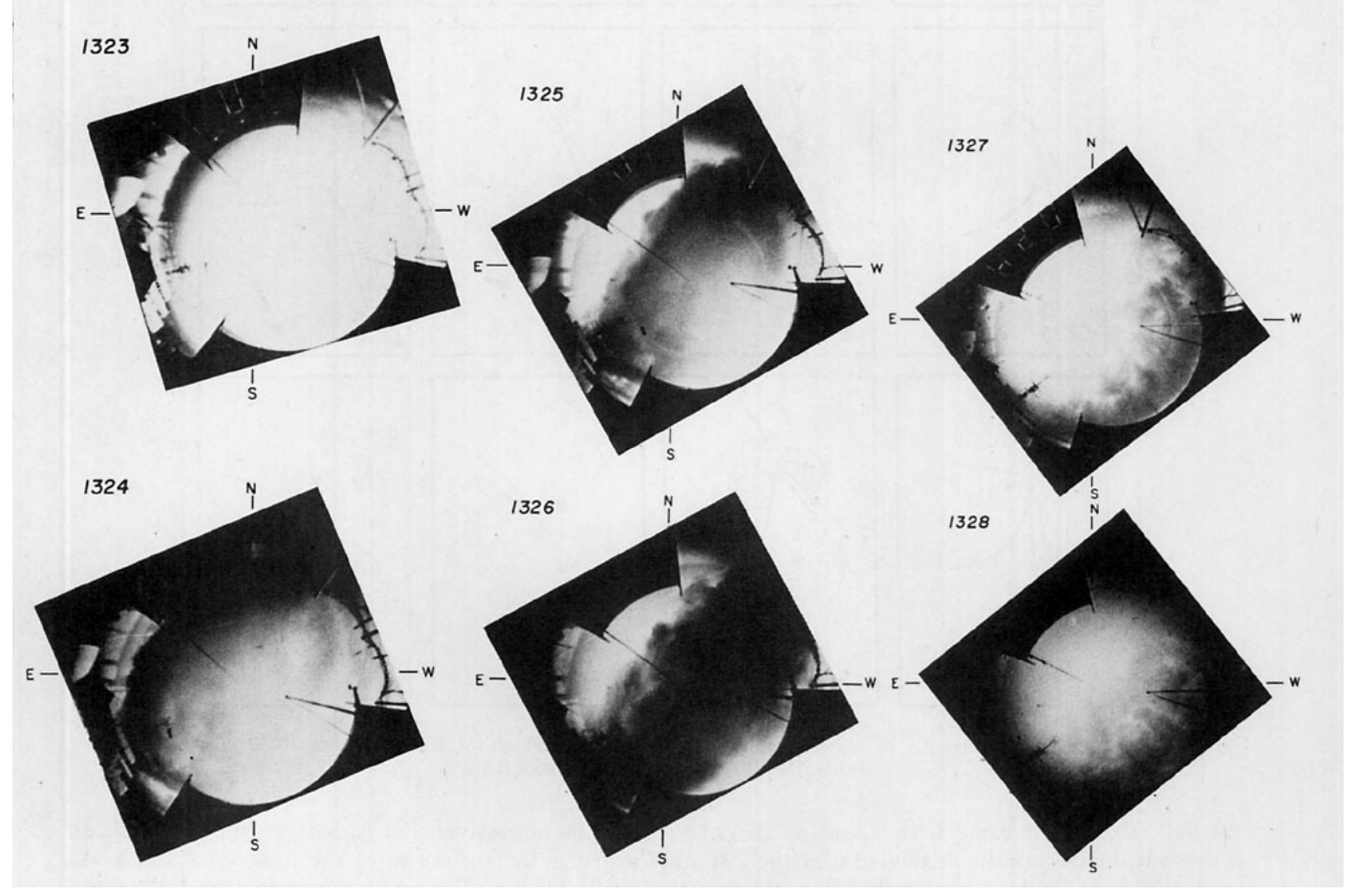


Fig. 22. Sequence of all-sky camera photographs taken on board the *Oceanographer*. Roll cloud appeared as dark feature centered on northeast horizon at 1323 GMT and was directly overhead at 1325–1326. By 1327–1328 only the back edge of the roll cloud was visible on the southwest horizon and raindrops were appearing on the camera lens as precipitation from LE 5 began at the ship.

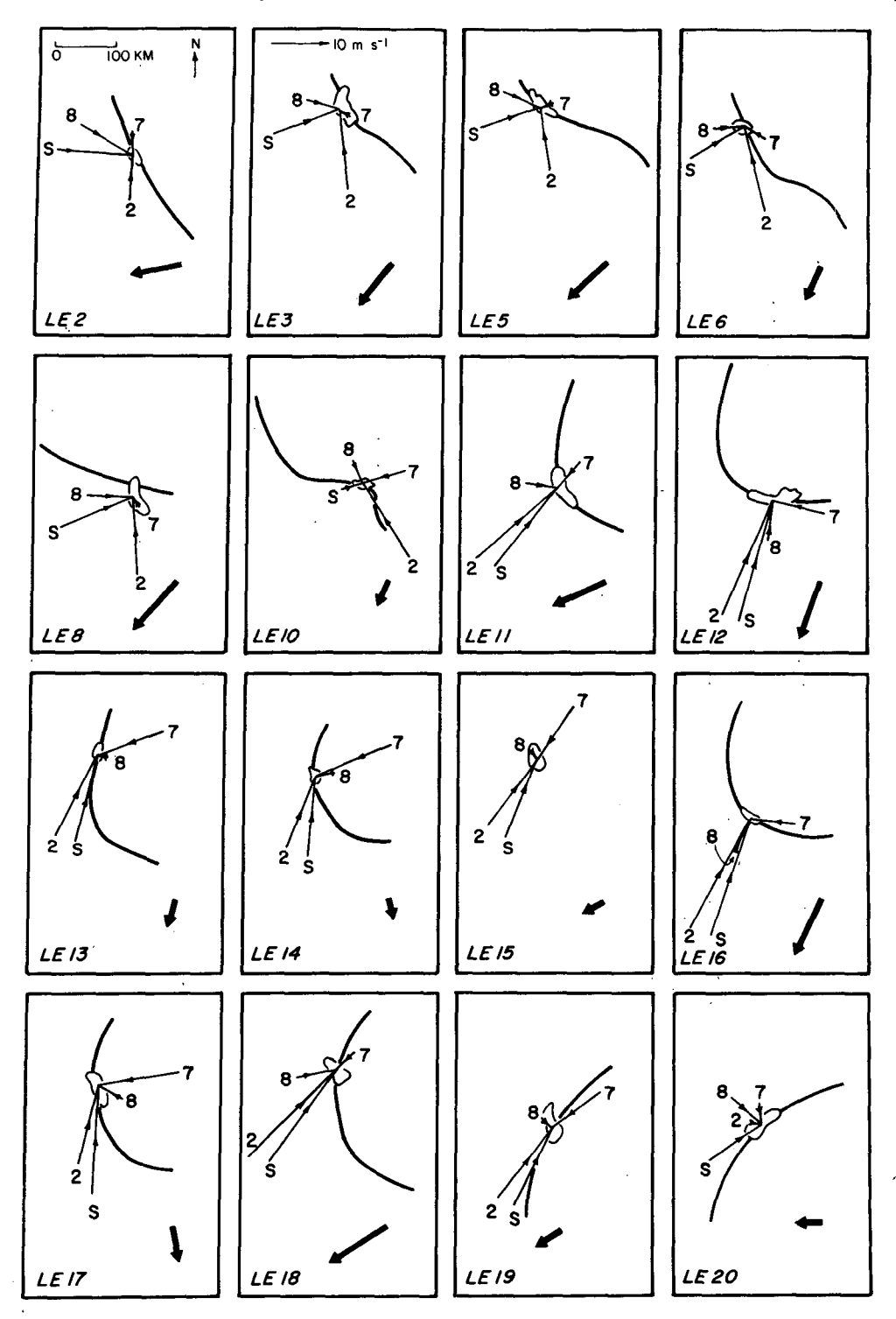


Fig. 23. Winds relative to individual LE's at the surface (S), 850 mb (8), 700 mb (7) and 200 mb (2) levels. Heavy arrows indicate velocities of LE's.

the 700 mb level it came from ahead of the LE's, whereas if the downdrafts originated near the 700 mb level, they were fed by a weak inflow from the rear of the elements.

The thermodynamic data in Figs. 8 and 10 show

that the lowest value of  $\theta_w$  observed in downdraft air reaching the surface after the passage of LE 5 was about 293.5 K. The convective-scale downdraft, therefore, either originated at about the 780 mb level or at the 400–500 mb level (Fig. 8, 1200 GMT sounding) and

sank undiluted to the sea surface, or the downdraft originated near the 700 mb level, where  $\theta_w \approx 291.5$  K (all soundings, Fig. 8) and was diluted by entrainment as the air sank. Since it is hard to imagine how the downdraft could have avoided entraining high- $\theta_w$  air from its neighboring updraft or from the general environment of the LE, the more likely altitude of downdraft origin for LE 5 was the 700 mb level, where, according to Fig. 23, the relative flow was weak but from the rear of the element.

In this respect, LE's 3 and 5 resembled all of the LE's in Fig. 23, which each had a 700 mb relative flow component parallel to the element's motion vector which was either weak or directed from the rear of the LE. It is therefore possible that the downdraft from each LE was fed from the rear of the LE at about the 700 mb level. The 850 and 700 mb winds often contained sizable components normal to the element's motion vector, indicating that much of the convective-scale downdraft air could have entered from the sides of the LE's.

In addition to their 700 mb relative flow, LE's 3 and 5 had other flow features in common with the other LE's. Each LE had a strong component of flow from ahead of the element at both the surface and 200 mb levels, while at the 850 mb level, the relative flow was not as strong but also had a component directed from ahead of the LE (Fig. 23).

### 14. Growth cycles of squall-line elements

The evolution of the maximum rainfall intensity and height of 21 LE's was studied by plotting RHI's similar to those in Figs. 19a and 19b along all radials (separated by 2° in azimuth) passing through each of the LE's at 15 min intervals throughout its lifetime. The evolution of the structure of each LE was examined in detail and summarized in diagrams such as those shown in Fig. 24 for LE's 3 and 5. The rainfall rate  $R(\text{mm h}^{-1})$  for the data points in Fig. 24 was computed from the radar reflectivity  $Z(\text{mm}^6 \text{ m}^{-3})$  using the relationship

$$Z = 230R^{1.25} \tag{1}$$

developed by Austin *et al.* (1976) from drop size data collected in GATE. The characteristics of all 21 LE's are summarized in Table 2.

From Fig. 24, it can be seen that the maximum height of LE's 3 and 5 progressed through a period of rapid growth, with echo tops "overshooting" the tropopause to a height of about 17 km, then decreasing in height to about 14 km, which corresponds to the top of the trailing anvil cloud with which the LE's merged at the end of their lifetimes. The maximum precipitation rate went through a period of rapid increase at first, but decreased considerably toward the end of the lifetime of each LE, so that the rainfall rate was relatively

Table 2. Characteristics of squall-line elements (LE's). Asterisks indicate that the values could not be determined. E means best estimate based on available information. Terms preceded by < or > are not included in averages.

LE no.	Time formed (GMT)	Time ended (GMT)	Lifetime (h)	Maximum height (km)	Final height (km)	Maximum point rainfall rate (mm h <sup>-1</sup> )	Maximum length (km)	Width at time of maximum length (km)
1	<0900	1000	>1	*	*	* '	*	*
2	0915	1100	1.75	17	11	47	50	30
3	0930	1215	2.75	17	14	166	70	45
4	0945	1215	2.50	17	16	81	70	20
5	0945	1500	5.25	17	14	>200	70	20
6	1030	1230	2.00	14	13	79	35	20
7	1045	1430	3.75	17	13	202	130	35
8	1145	1430	E3.25	17	12	70	75	45
9	1245	E1345	E1.00	16	*	55	E30	E15
10	1315	E1500	E1.75	*	*	*	E50	E30
11	1400	1630	2.50	17	16	79	85	55
12	1430	1815	3.25	15	11	83	90	20
13	1430	1645	2.25	15	11	134	40	20
14	1500	1630	1.50	17	14	85	40	20
15	1515	1830	3.00	16	14	94	70	30
16	1545	>1800	>2.25	10	E10	139	40	15
17	1545	1800	2,25	17	16	234	50	E20
18	1730	E2000	E2.50	18	17	77	80	30
19	1800	E2015	E2.25	17	*	87	60	30
20	2215	2400	1.75	16	10	139	60	20
21	2330	2400	0.50	10	*	117	35	10
Average			2.4	16	13	109	60	25

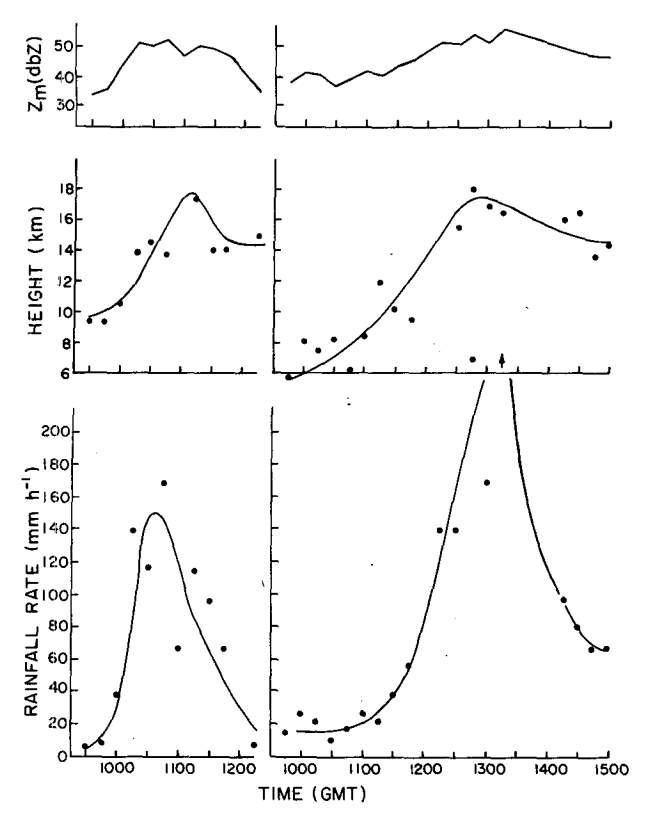


Fig. 24. Maximum radar reflectivity  $(Z_m)$ , echo height and surface rainfall rate as functions of time determined by tracking three-dimensional echoes associated with LE's 3 and 5.

low as the LE merged with the trailing anvil precipitation region.

Most of the LE's followed growth cycles similar to those of LE's 3 and 5. On average, LE's reached maximum heights of 16 km, were 13.5 km in height when they merged with the trailing anvil region, had maximum rainfall rates of a little over 100 mm h<sup>-1</sup>, and attained horizontal dimensions of 65 km×30 km (Table 2). The LE's had similar durations but reached greater maximum heights than average GATE radar

echoes in their horizontal size range (Houze and Cheng, 1977).

# 15. Structure of the trailing anvil region

Unlike the deep convective cores comprising the squall line itself, the anvil region of the squall-line system was horizontally stratified (Fig. 25). The pronounced bright band of radar reflectivity seen near the melting level is a characteristic feature of stratiform precipitation, and it appeared in virtually every cross section through the anvil region. The bright band in Fig. 25 slopes slightly, being higher toward the squall line and lower toward the rear (northeast side) of the system. Interpreted as a 0° isotherm, the sloping bright band indicates that a horizontal temperature gradient extended across the squall-line system in the middle troposphere, with cooler air located toward the rear of the squall line. Evaporation of precipitation particles falling below the base of the anvil cloud (Fig. 2) probably led to the lower temperatures toward the rear of the system. Evaporation also apparently resulted in the absence of precipitation particles in the lower troposphere, with the consequent observation of overhanging precipitation (virga) that was falling from the anvil cloud but not reaching the sea surface at the northeastern boundary of the stratiform echo zone (Fig. 25).

The radar reflectivity pattern in the anvil region is consistent with the wind and thermodynamic patterns of Figs. 10–13 which indicate that a broad region of cool downdraft air was located below the anvil cloud. This downdraft was mesoscale and, therefore, distinctly different from the convective-scale downdrafts associated with individual LE's. Brown's (1974) results suggest that the mesoscale downdraft is a hydrostatic feature, thermally driven by cooling due to the evaporation of precipitation falling from the anvil cloud. The pronounced melting band seen in Fig. 25 indicates [as noted by Zipser (1977)] that the melting of ice particles

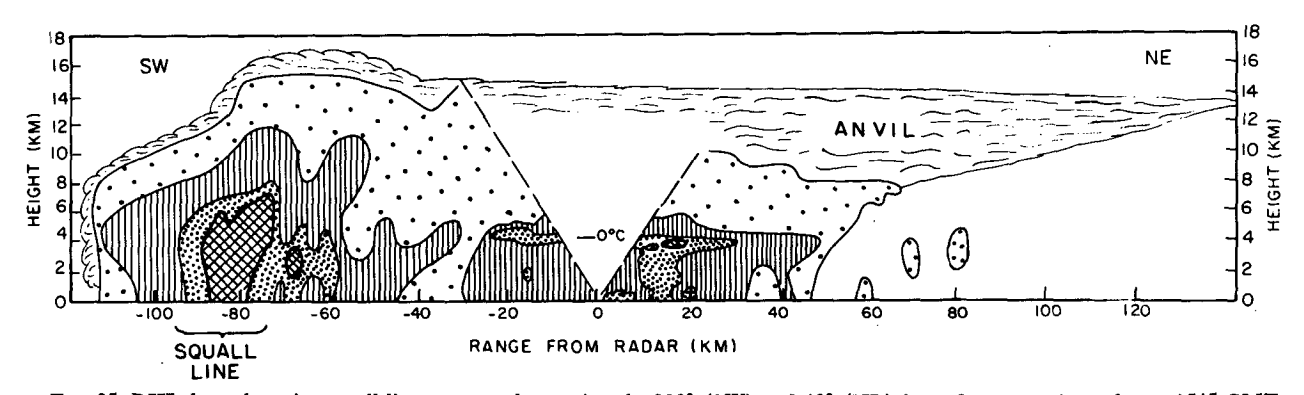


Fig. 25. RHI through entire squall-line system, along azimuths 223° (SW) and 43° (NE) from *Oceanographer* radar at 1545 GMT 4 September 1974 (see Fig. 17j). Inside contours are for 38, 33, 23 dBZ and minimum detectable echo. Outside scalloped contour outlines cloud boundary estimated from infrared satellite imagery.

also contributes substantially to the cooling in the mesoscale downdraft.

The vertical velocity in the mesoscale downdraft was estimated by Zipser (1977) and found in Brown's (1974) model to be  $\sim 10$  cm s<sup>-1</sup>, while convective-scale downdrafts are typically  $\sim 1$ –10 m s<sup>-1</sup>. As discussed in Section 7 and indicated in Fig. 2, the mesoscale downdraft apparently helped maintain the stable layer at the top of the surface layer of outflowing convective-scale downdraft air just a few hundred meters above the sea surface.

### 16. Squall-line and anvil precipitation

On maps showing the radar reflectivity in 4 km × 4 km horizontal grid spaces over the entire GATE radar area (Section 8), the squall line and anvil regions of the 4-5 September squall-line system were identified. The position of the squall line was indicated roughly by the arrows in Figs. 15a-15j. For computational purposes, a boundary was drawn around the squall line. The portion of the squall-line system outside this boundary was considered to be the anvil region. Since the anvil region was connected to the trailing edge of the squall line, the rear boundary of the squall line region was somewhat arbitrary. Generally, however, the rear boundary seemed to follow the 29 dBZ radar reflectivity (or 3 mm h<sup>-1</sup> rainfall rate) contour. Eq. (1) was used to convert the radar reflectivity in each grid square to rainfall rate. The grid-square values of rainfall rate were integrated with respect to area over the regions contained within the squall-line and anvil boundaries for each radar map time. The results are shown in Fig. 26, which compares the area-integrated rainfall rates in the squall-line and anvil regions.

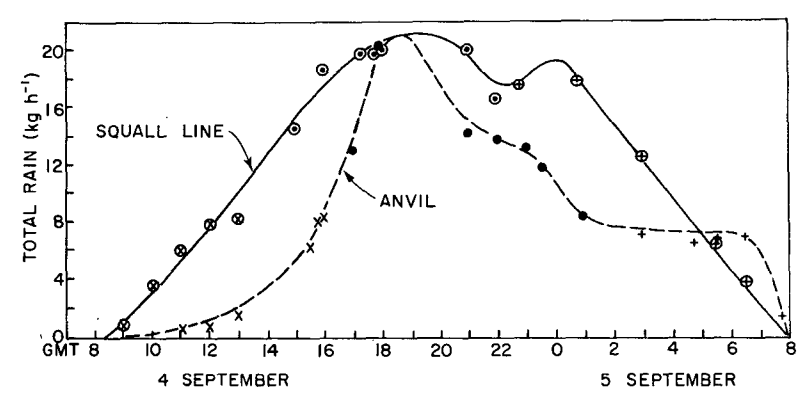
From Fig. 26, it can be seen that in the early stages of the squall-line system (0900-1300) a relatively small amount of precipitation fell in the anvil region. This rain was contained in small patches of precipitation

under the developing anvil cloud (Figs. 15a–15d). By 1500, however, the anvil precipitation zone had spread over a large area behind the squall line (Fig. 15e). By 1900 (Fig. 15g), the amount of rain falling from the anvil cloud was approximately equal to that coming from the squall line itself (Fig. 26). Integration of the curves in Fig. 26 over the lifetime of the squall-line system (0900 4 September–0800 5 September) shows that  $1.8 \times 10^{12}$  kg of rainwater fell from the area covered by the anvil, while  $2.8 \times 10^{12}$  kg fell from the area covered by the squall line itself. Thus, about 40% of the precipitation from the squall-line system fell from the trailing anvil cloud.

It seems unlikely that so much rain could have fallen from an anvil cloud consisting of a shallow layer of dynamically inactive debris blown off the tops of the cumulonimbus elements forming the squall line. The anvil cloud, therefore, was dynamically active or it evolved from a deeper layer of squall-line debris. Both hypotheses seem plausible.

First, it is possible that the anvil cloud began as inactive debris blowing away from the top of the squall line. Then, as in Brown's (1974) numerical model, widespread lifting developed throughout the upper level anvil cloud and produced substantial amounts of additional precipitation which subsequently fell through the base of the anvil cloud.

Second, the successive incorporation of old LE's into the anvil region (Sections 9 and 14) could account for the observed large amounts of rain that fell from the anvil cloud. As each old LE weakened, the sudden cessation of the updrafts producing the LE must have left large quantities of water aloft, at all altitudes below cloud top. This water, however, did not fall out until after the old LE was incorporated into the anvil region to the rear of the squall line. This idea is consistent with Kessler's (1969) kinematic cloud models which show that the sudden cessation of a strong up-



Frg. 26. Total rain integrated over areas covered by squall line and anvil portions of the squall-line system. Circled points refer to squall line region. Data points derived from *Oceanographer* radar echo patterns are indicated by X's. Points derived from composite *Oceanographer* and *Researcher* radar echo patterns indicated by dots. Points derived from composite *Oceanographer*, *Researcher* and *Gilliss* echo patterns are indicated by crosses.

draft is followed by a rapid rise in cloud base due to collection of all the cloud-sized droplets at low levels by the larger precipitation particles. A dissipated but precipitation-laden LE would therefore have developed a middle or upper level cloud base, rendering it indistinguishable from the rest of the anvil structure behind the squall line (Fig. 2).

### 17. Conclusions

On 4–5 September 1974, a tropical squall-line system (Fig. 2) formed and moved through the GATE data network between the upstream trough and downstream ridge of an African wave. During its 23 h lifetime, the squall-line system displayed a relative airflow pattern that was similar in its general characteristics to squall-line flow patterns described previously by Hamilton and Archbold (1945), Zipser (1969, 1977), Obasi, (1974) and Betts et al. (1976).

The squall line itself, which formed the leading edge of the squall-line system, consisted of discrete active centers of cumulonimbus convection, here referred to as squall-line elements or LE's. New LE's systematically formed ahead of the squall line which was composed of heavily precipitating mature LE's. Old LE's blended into the stratiform anvil region behind the squall line as they weakened. The intensity of the updrafts in mature LE's was so great that their tops penetrated the tropopause level and maximum cloud tops reached heights of 16–17 km along the squall line.

The downpour of heavy precipitation below the sloping updraft contained a convective-scale downdraft in the heavy rain zone which spread out at low levels. One portion of this cold air spread toward the front of the system and produced the squall front just ahead of the heavy precipitation region and another portion streamed out of the trailing side of the system in a thin layer just above the sea surface. The convective-scale downdraft was followed by a mesoscale downdraft occupying the region below the trailing anvil cloud. The layer of cold, convective-scale downdraft air streaming out toward the trailing edge of the system was separated from the mesoscale downdraft air above it by a stable layer at a height of 200-400 m above the sea surface.

The precipitation falling from the trailing anvil cloud was stratiform in character, a fact that was emphasized by the pronounced bright band of high radar reflectivity which extended through the anvil precipitation region. The stratiform rain that fell from the anvil cloud accounted for 40% of the total rainfall from the entire squall-line system. This percentage appears to be greater than what could reasonably have been expected if the anvil was simply inactive debris blowing off the tops of the cumulonimbus elements comprising the squall line. The large amount of rain falling from the anvil may have resulted from the successive incorporation of precipitation-laden old squall-line ele-

ments into the anvil region as they weakened toward the rear of the squall line or from mesoscale ascent throughout the anvil cloud, as predicted by Brown's (1974) model.

The detailed examination of the cloud and precipitation fields associated with the 4-5 September squallline system and the analysis of the air motions associated with the disturbance presented in this paper provide insight into squall-line dynamics which can now be used to guide the development and refinement of models for evaluating quantitatively the effect of this type of tropical convection on the larger scale environment. One of the primary objectives of GATE was to measure the impact of deep tropical convective systems on the large-scale atmospheric motions, and the next step in the analysis of the 4-5 September squall-line system is to adapt the models developed by Austin and Houze (1973), Houze (1973) and Houze and Leary (1976) to the squall-line situation. Vertical transports of mass, heat and momentum accomplished by the squall-line system will be computed using the GATE radar data as input to the model calculations.

Acknowledgments. The author appreciates the interest of Dr. Edward J. Zipser who arranged for the author to visit the NCAR Group during the course of this study. Professor Richard J. Reed and Ms. Colleen Leary read the manuscript and made helpful comments. Ms. Leary and Mr. John Gamache developed software for plotting and analyzing the GATE digital radar data on the University of Washington computer system. Mr. Leigh Matheson assisted in much of the data analysis and reduction. The following GATE scientists provided the author with data: Dr. Geoffrey L. Austin, Dr. Pauline M. Austin, Mr. Gordon Dean, Dr. John E. Gaynor, Mr. Spiros G. Geotis, Dr. Michael D. Hudlow, Mr. Ron Holle, Mr. Frank D. Marks, Dr. David W. Martin, Mr. Steven W. Payne, Professor Richard J. Reed, Dr. David Suchman and Dr. Edward J. Zipser. The figures were drafted by Mrs. Kay Moore.

This research was supported by the Global Atmospheric Research Program, National Science Foundation, and the U. S. GATE Project Office under Grant ATM 74-14830 A01.

#### REFERENCES

- Acheson, D., 1976: Documentation for GATE B-scale rawinsondes. GATE Processed and Validated Data,\* 21 pp.
- Austin, G. L., 1977: Documentation for radar. Quadra microfilm data set. GATE Processed and Validated Data,\* 3 pp.
- Austin, P. M., 1976a: Documentation for Gilliss radar raw digital data. GATE Processed and Validated Data,\* 50 pp.
- —, 1976b: Documentation for Gilliss radar images on 35 mm film. GATE Processed and Validated Data,\* 65-74.
- —, 1976c: Documentation for Gilliss radar Cartesian hybrid data set. GATE Processed and Validated Data,\* 79 pp.
- —, and R. A. Houze, Jr., 1973: A technique for computing vertical transports by precipitating cumuli. J. Atmos. Sci., 30, 1100-1111.

- —, S. Geotis, J. Cunning, J. Thomas, T. R. Sax and J. Gillespie, 1976: Raindrop size distributions and Z-R relationships for GATE. Paper presented at the Tenth Technical Conference on Hurricanes and Tropical Meteorology, Charlottesville, Amer. Meteor. Soc. [Abstract in Bull. Amer. Meteor. Soc., 57, 518.]
- Betts, A. K., R. W. Grover and M. W. Moncrieff, 1976: Structure and motion of tropical squall-lines over Venezuela. Quart. J. Roy. Meteor. Soc., 102, 395-404.
- Brooks, C. F., 1922: The local, or heat, thunderstorm. Mon. Wea. Rev., 50, 281-287.
- Brown, J. M., 1974: Mesoscale motions induced by cumulus convection: a numerical study. Ph.D. thesis, MIT, 206 pp.
- Browning, K. A., J. C. Fankhauser, J.-P. Chalon, P. J. Eccles,
  R. G. Strauch, F. H. Merrem, D. J. Musil, E. L. May and
  W. R. Sand, 1976: Structure of an evolving hailstorm, Part V:
  Synthesis and implications for hail growth and hail suppression. Mon. Wea. Rev., 104, 603-610.
- Burpee, R. W., 1972: The origin and structure of easterly waves in the lower troposphere in North Africa. J. Atmos. Sci., 29, 77-90.
- ——,1974: Characteristics of North African easterly waves during the summers of 1968 and 1969. J. Atmos. Sci., 31, 1556-1570.
- —, 1975: Some features of synoptic-scale waves based on compositing analysis of GATE data. Mon. Wea. Rev., 103, 921-925
- Byers, H. R., and R. R. Braham, Jr., 1949: The Thunderstorm. U. S. Weather Bureau, Washington, D. C., 287 pp.
- Carlson, T. N., 1969a: Synoptic histories of three African disturbances that developed into Atlantic hurricanes. Mon. Wea. Rev., 97, 256-276.
- —, 1969b: Some remarks on African disturbances and their progress over the tropical Atlantic. *Mon. Wea. Rev.*, 97, 716–726.
- Dennis, A. S., C. A. Schock and A. Koscielski, 1970: Characteristics of hailstorms of western South Dakota. J. Appl. Meteor. 9, 127-135.
- EDS, 1975: GATE Data Catalogue. Environmental Data Service, NOAA, Washington, D. C.
- Eldridge, R. H., 1957: A synoptic study of West African disturbance lines. Quart. J. Roy. Meteor. Soc., 83, 303-314.
- Hamilton, R. A., and J. W. Archbold, 1945: Meteorology of Nigeria and adjacent territory. Quart. J. Roy. Meteor. Soc., 71, 231-262.
- Houze, R. A., Jr., 1973: A climatological study of vertical transports by precipitating cumuli. J. Atmos. Sci., 30, 1112-1123.
- —, 1975: Squall lines observed in the vicinity of the Researcher during Phase III of GATE. Preprints 16th Radar Meteorology Conf., Houston, Amer. Meteor. Soc., 206-209.
- —, 1976: GATE radar observations of a tropical squall line. Preprints 17th Conf. Radar Meteorology, Seattle, Amer. Meteor. Soc., 384-389.
- —, and C.-P. Cheng, 1977: Radar characteristics of tropical convection observed during GATE: Mean properties and trends over the summer season. Mon. Wea. Rev., 105, 964-980.
- —, and C. A. Leary, 1976: Comparison of convective mass and heat transports in tropical easterly waves computed by two methods. J. Atmos. Sci., 33, 424-429.
- Hudlow, M. D., 1975a: Collection and handling of GATE ship-board radar data. Preprints 16th Radar Meteorology Conf., Houston, Amer. Meteor. Soc., 186-193.
- ---, 1975b: Documentation for GATE Oceanographer Radar Film. GATE Processed and Validated Data,\* 50 pp.
- —, 1976a: Documentation for GATE NOAA hybrid microfilm graphics data. GATE Processed and Validated Data,\* 12 pp.

- ---, 1976b: Documentation for GATE NOAA hybrid data, GATE Processed and Validated Data,\* 31 pp.
- —, 1976c: Documentation for Researcher radar images on 35 mm microfilm. GATE Processed and Validated Data,\* 18 pp.
- Humphries, W. J., 1914: The thunderstorm and its phenomena. Mon. Wea. Rev., 42, 348-380.
- Kessler, E., 1969: On the distribution and continuity of water substance in atmospheric circulations. *Meteor. Monogr.*, No. 32, 84 pp.
- Lienesch, J. H., 1975: Corrections of VISSR data obtained during GATE. Memo. Nat. Environ. Satellite Service, NOAA, Washington, D. C., 6 pp.
- Mandics, P. A., and F. F. Hall, Jr., 1976: Preliminary results from the GATE acoustic echo sounder. Bull. Meteor. Soc., 57, 1142-1147.
- ——, ——, E. J. Owens and D. Wylie, 1975: Observations of the tropical marine atmosphere using an acoustic echo sounder during GATE. Preprints 16th Radar Meteor. Conf., Houston, Amer. Meteor. Soc., 257–259.
- Miller, M. J. and R. P. Pearce, 1974: A three-dimensional primitive equation model of cumulonimbus convection. Quart. J. Roy. Meteor. Soc., 100, 133-154.
- —, and A. K. Betts, 1977: Traveling convective storms over Venezuela. Mon. Wea. Rev., 105, 833-848.
- Moncrieff, M. W. and M. J. Miller, 1976: The dynamics and simulation of tropical cumulonimbus and squall lines. Quart. J. Roy. Meteor. Soc., 102, 373-394.
- Obasi, G. O. P., 1974: The environmental structure of the atmosphere near West African disturbance lines. *Preprints Int. Tropical Meteorology Meeting*, Nairobi, Kenya, Part II, Amer. Meteor. Soc., 62-66.
- Ogura, Y., and T. Takahashi, 1971: Numerical simulation of the life cycle of a thunderstorm cell. Mon. Wea. Rev., 99, 895-911.
- Payne, S. W., and M. M. McGarry, 1977: The relationship of satellite inferred convective activity to easterly waves over West Africa and the adjacent ocean during Phase III of GATE. Mon. Wea. Rev., 105, 413-420.
- Reed, R. J., D. C. Norquist and E. E. Recker, 1977: The structure and properties of African wave disturbances as observed during Phase III of GATE. Mon. Wea. Rev., 105, 317-333.
- Roll, H. U., 1965: Physics of the Marine Atmosphere. Academic Press, 426 pp.
- Rosenthal, S. L., 1977: Numerical simulation of tropical cyclone development with latent heat release by the resolvable scales. II: Propagating small-scale features observed in the pre-hurricane phase. Manuscript in preparation.
- Takeda, T., 1971: Numerical simulation of a precipitating convective cloud: The formation of a "long-lasting" cloud. J. Atmos. Sci., 28, 350-376.
- Tschirhart, G., 1958: Les conditions aérologiques à l'avant des lignes de grains en Afrique Equatoriale. Météor. Nationale, Mono. No. 11, 28 pp.
- Wilhelmson, R., 1974: The life cycle of a thunderstorm in three dimensions. J. Atmos. Sci., 31, 1629-1651.
- Zipser, E. J., 1969: The role of organized unsaturated convective downdrafts in the structure and rapid decay of an equatorial disturbance. J. Appl. Meteor., 8, 799-814.
- —, 1977: Mesoscale and convective-scale downdrafts as distinct components of squall-line circulation. Mon. Wea. Rev., 105, 1568-1589.

<sup>\*</sup> Available from World Data Center-A, National Climatic Center, Asheville, N. C.